Freie Universität Berlin
Fachbereich Mathematik und Informatik
Studiengang Mathematik

Masterarbeit

Grad-div Stabilization for Incompressible Stokes Equations

Vorgelegt von: Xiaoguo Lu
Matrikelnummer: 5284213
Erstgutachter: Univ.-Prof. Dr. Volker John
Zweitgutachter: PD Dr. Alfonso Caiazzo
Ort und Datum: Berlin, May 18, 2023

Statutory Declaration

I declare that I have developed and written the enclosed Master's thesis completely by myself, and have not used sources or means without declaration in the text. Any thoughts from others or literal quotations are clearly marked. The Master's thesis was not used in the same or in a similar version to achieve an academic grading or is being published elsewhere.

Berlin (Germany), May 18, 2023

Xiaoguo Lu 18.05.2023

Acknowledgements

My sincere and heartfelt gratitude goes firstly to my supervisor Univ.-Prof. Dr.Volker John, for his strong sense of responsibility, patience, encouragement, constructive feedback, insightful suggestions, and careful guidance throughout the progress of my thesis. His professional mathematical understanding and ability have greatly enriched my academic journey. It is truly grateful for the opportunity to be guided by such an exceptional educator and mentor.
Furthermore, I would like to express my sincere appreciation to PD Dr. Alfonso Caiazzo for being the second supervisor of my thesis.
Finally, I want to extend my thanks to my family and friends for their love and support throughout my journey of studying in a foreign land, particularly during the difficult period of the pandemic.

Contents

Chapter 1

Introduction

1.1 Motivation

The incompressible Stokes equations are a fundamental model in fluid mechanics, describing the motion of viscous fluids in the absence of external forces. They consist of the conservation of mass equation and the momentum equation and play an essential role in understanding a wide range of fluid flows. However, the numerical solution to these equations is challenging. One aspect is that pairs of velocity and pressure finite element spaces that lead to well-posed problems lead simultaneously to solutions that violate the conservation of mass.

The grad-div stabilization method is an effective approach to address this issue, as it reduces the divergence of velocity and enhances the mass conservation properties, resulting in a more accurate numerical solution. This method is typically applied in the Taylor-Hood finite element space, which consists of continuous piecewise polynomial functions for velocity and pressure. The effectiveness of this method is highly dependent on the choice of stabilization parameter. Furthermore, the value of viscosity also has an impact on the numerical solution.

In this thesis, we investigate the application of grad-div stabilization to the incompressible Stokes equations, with a focus on its impact on the accuracy and mass conservation properties of the numerical solutions. We provide error estimates for different grad-div stabilization methods in the Taylor-Hood finite element space, to compare their performance. Additionally, we analyze the effect of the different factors on the numerical solutions.

1.2 Structure

This thesis is organized as follows:

- Chapter 2 begins with a physical derivation of the incompressible Navier-Stokes equations and their non-dimensionalization for numerical analysis. The Stokes equations are also introduced.

- Chapter 3 starts with the weak formulation of the Stokes equations, followed by the inf-sup condition and the construction of finite element spaces. A detailed explanation of the Galerkin finite element method and standard error analysis is also provided. Then, an example of the inf-sup stable pairs on finite element spaces, specifically the Taylor-Hood elements, is given which will be used as the basis for the numerical experiments in later chapters.

- Chapter 4 introduces two grad-div stabilization methods, namely the standard and sparse methods, with a summary of the properties of the sparse method. The impact of these methods on the accuracy of the finite element solution and the convergence properties of the Taylor-Hood finite element space is analyzed.

- Chapter 5 presents the results of several numerical experiments conducted on 2D and 3D examples. The experiments focus on three main aspects: the performance of different grad-div stabilization methods, the impact of varying degrees of the Taylor-Hood spaces, and the influence of different values of viscosity. Furthermore, the efficiency of two grad-div stabilization methods is compared in a 3D example.

- Chapter 6 concludes with a discussion of the main findings and potential future research directions.

Chapter 2

Incompressible Navier-Stokes Equations and their Finite Element Discretization

2.1 Derivation of Navier-Stokes Equations

Fluid mechanics has numerous applications in fields such as environmental science, marine engineering, and atmospheric science. The Navier-Stokes equations, which were introduced in the 19th century, are dynamic conservation equations used to describe viscous incompressible fluids. The equations can be derived from the fundamental principles of conservation of mass and momentum.

2.1.1 The Conservation of Mass

Remark 2.1.1 (The conservation of mass) Consider a control volume $\Omega \subset R^d, d = 2, 3$, with a sufficiently smooth surface $\partial\Omega$, the flow velocity vector is $\boldsymbol{v}(t, \boldsymbol{x})$ and density is $\rho(t, \boldsymbol{x})$. According to the conservation of mass, it states that the change of mass in time plus the flow of mass through the boundary equals 0,

$$\frac{\partial}{\partial t}\int_{\Omega} \rho d\Omega + \int_{\partial\Omega} \rho \boldsymbol{v} \cdot \boldsymbol{n} dS = 0, \tag{2.1.1}$$

where $\boldsymbol{n}$ is the outward pointing unit normal on $S \in \partial\Omega$.
Since all functions and $\partial\Omega$ are assumed to be sufficiently smooth, we can apply the divergence theorem to transform a surface integral into a volume integral. The divergence theorem states that:

$$\int_{\Omega} \nabla \cdot (\rho \boldsymbol{v}) d\Omega = \int_{\partial\Omega} \rho \boldsymbol{v} \cdot \boldsymbol{n} dS. \tag{2.1.2}$$

So the final differential form can be written as

$$\int_{\Omega} \left(\partial_t \rho + \nabla \cdot (\rho \boldsymbol{v})\right) d\Omega = 0. \tag{2.1.3}$$

Since the choice of Ω is arbitrary, then (2.1.3) becomes

$$\partial_t \rho + \nabla \cdot (\rho \boldsymbol{v}) = 0. \tag{2.1.4}$$

This equation (2.1.4) is the differential form of the conservation of mass, also known as the continuity equation for fluids. $\square$

Remark 2.1.2 (Incompressible, Homogeneous Fluids) Assuming that the fluid is incompressible and homogeneous, meaning that its density remains constant and is represented as $\rho_0 > 0$, it can be observed by expanding the divergence operator in equation (2.1.4) that the velocity divergence is zero as follows

$$\nabla \cdot \boldsymbol{v} = (\partial_x v_1 + \partial_y v_2 + \partial_z v_3)(t, \boldsymbol{x}) = 0, \tag{2.1.5}$$

where $\boldsymbol{v} = (v_1, v_2, v_3)$. On the other hand, the divergence of velocity is 0, if the fluid is incompressible and homogeneous. $\square$

Remark 2.1.3 (Time-Dependent Domain) Let $F(\boldsymbol{x}, t)$ be some field variable defined as a function of space and time, $\Omega(t)$ be a time-dependent control volume that encloses some finite region in space at each instant of time, the time-dependent surface of the control volume is S, then the Reynolds transport theorem has the form

$$\frac{d}{dt} \int_{\Omega(t)} F d\Omega = \int_{\Omega(t)} \partial_t F d\Omega + \int_{\partial\Omega(t)} F \boldsymbol{v} \cdot \boldsymbol{n} dS. \tag{2.1.6}$$

Let $F = \rho$, where ρ is the density of the fluid. The conservation of mass and the divergence theorem gives

$$\frac{d}{dt} \int_{\Omega(t)} \rho d\Omega = \int_{\Omega(t)} \left(\partial_t \rho d\Omega + \nabla \cdot (\rho \boldsymbol{v})\right) d\Omega. \tag{2.1.7}$$

The left-hand side of the equation is the rate of change of the total mass inside the control volume. If there is no source of mass within the control volume, the left-hand side of the equation must equal zero. Since the choice of the control volume is arbitrary, the kernel of the right-hand side of the equation must therefore equal to zero at every point in the flow. Thus the continuity equation in the absence of mass sources has the same form as (2.1.4). $\square$

2.1.2 The Conservation of Momentum

Remark 2.1.4 (Conservation of Momentum) Newton's second law states

the rate of a change of momentum = force = mass × acceleration.

By the conservation of momentum, it reformulates as

$$\frac{\partial}{\partial t}\int_{\Omega} \rho \boldsymbol{v} d\Omega + \int_{\partial\Omega} (\rho \boldsymbol{v})(\boldsymbol{v} \cdot \boldsymbol{n}) dS = \int_{\partial\Omega} \boldsymbol{T} dS + \int_{\Omega} f_b d\Omega, \tag{2.1.8}$$

where f_b is the body force, σ is the symmetric Cauchy stress tensor, and $\boldsymbol{T}$ is the stress vector, $\boldsymbol{T} = \boldsymbol{n} \cdot \sigma$, depending on the outward pointing unit normal vector $\boldsymbol{n}$. Applying Reynolds' transport theorem and divergence theorem, then

$$\int_{\Omega} \rho(\partial_t \boldsymbol{v} + (\boldsymbol{v} \cdot \nabla)\boldsymbol{v} d\Omega = \int_{\Omega} \nabla \cdot \sigma d\Omega + \int_{\Omega} f_b d\Omega. \tag{2.1.9}$$

Since Ω is arbitrary, we have

$$\rho(\partial_t \boldsymbol{v} + (\boldsymbol{v} \cdot \nabla)\boldsymbol{v}) = \nabla \cdot \sigma + f_b. \tag{2.1.10}$$

□

Remark 2.1.5 (Decomposition of the Cauchy Stress Tensor) The Cauchy stress tensor can be decomposed into the isotropic part and anisotropic part:

$$\sigma = -P\boldsymbol{I} + \tau, \tag{2.1.11}$$

where trace$(\tau) = 0$, the pressure is defined as P. The parameter τ usually depends on the rate of strains and the spatial derivative of velocity. In the case of a Newtonian fluid,

$$\tau = \mu(\nabla \boldsymbol{v} + \nabla \boldsymbol{v}^T), \tag{2.1.12}$$

where μ is the viscosity, then (2.1.10) is reduced to

$$\rho(\partial_t \boldsymbol{v} + (\boldsymbol{v} \cdot \nabla)\boldsymbol{v}) = -\nabla P + \mu \triangle \boldsymbol{v} + f_b. \tag{2.1.13}$$

Assume the parameters μ and ρ are positive constants, the Navier-Stokes equations are

$$\begin{aligned} \partial_t \boldsymbol{v} - \nu \triangle \boldsymbol{v} + (\boldsymbol{v} \cdot \nabla)\boldsymbol{v} + \nabla \frac{P}{\rho} &= \frac{f_b}{\rho}, \\ \nabla \cdot \boldsymbol{v} &= 0, \end{aligned} \tag{2.1.14}$$

where $\nu = \mu/\rho$ is the kinematic viscosity of the fluid. □

2.1.3 Dimensionless Equations

Dimensionless quantities make it easier to define scales in some cases, such as Navier-Stokes equations, which allow us to derive physical meaning more easily. In addition, they are well suited for numerical simulations, see [1].

Remark 2.1.6 (The Navier–Stokes Equations in Dimensionless Form) With length scale L, time scale T and velocity scale U, the dimensionless variables are introduce as following

$$\boldsymbol{v}' = \frac{\boldsymbol{v}}{U}, \quad t' = \frac{t}{T}, \quad \boldsymbol{x}' = \frac{\boldsymbol{x}}{L}. \tag{2.1.15}$$

The Navier-Stokes equations (2.1.14) become

$$\begin{aligned} \frac{L}{TU}\partial_t \boldsymbol{v}' - \frac{2\nu}{UL}\triangle \boldsymbol{v}' + (\boldsymbol{v}' \cdot \nabla)\boldsymbol{v}' + \frac{1}{\rho U^2}\nabla P = \frac{L}{\rho U^2} f_b, \\ \nabla \cdot \boldsymbol{v}' = 0. \end{aligned} \tag{2.1.16}$$

Define the Strouhal number and Reynolds number

$$\begin{aligned} \frac{L}{TU} &= \text{Strouhal numer} = St, \\ \frac{UL}{\nu} &= \text{Reynolds number} = Re, \end{aligned} \tag{2.1.17}$$

and introduce pressure and body force scales as

$$p = \frac{P}{\rho U^2}, \quad f = \frac{L}{\rho U^2} f_b. \tag{2.1.18}$$

For simplicity of notation, the variables are renamed again. With $x' = x$, $t' = t$, $v' = u$, one gets the dimensionless Navier-Stokes equations

$$\begin{aligned} St\partial_t \boldsymbol{u} - \frac{1}{Re}\triangle \boldsymbol{u} + (\boldsymbol{u} \cdot \nabla)\boldsymbol{u} + \nabla p = f, \\ \nabla \cdot \boldsymbol{u} = 0. \end{aligned} \tag{2.1.19}$$

In order to simplify (2.1.19) again, one chooses the characteristic time scale $T = L/U$ and $\nu = Re^{-1}$, then gets

$$\begin{aligned} \partial_t \boldsymbol{u} - \nu \triangle \boldsymbol{u} + (\boldsymbol{u} \cdot \nabla)\boldsymbol{u} + \nabla p = f, \\ \nabla \cdot \boldsymbol{u} = 0. \end{aligned} \tag{2.1.20}$$

□

2.1.4 Special Cases for Incompressible Flow

Remark 2.1.7 (Steady-State Navier-Stokes Equation) The flow of a fluid is steady if its velocity and pressure are independent of the time at every point in the flow field. Hence one can skip the time derivative to get the steady-state Navier-Stokes equations as follows

$$\begin{aligned} -\nu\triangle\boldsymbol{u} + (\boldsymbol{u}\cdot\nabla)\boldsymbol{u} + \nabla p &= f, \\ \nabla\cdot\boldsymbol{u} &= 0. \end{aligned} \tag{2.1.21}$$

□

Remark 2.1.8 (Stokes Equation) The Stokes equations describe the flow of a viscous and incompressible fluid at small Reynolds numbers, which can be obtained by neglecting the nonlinear convection term in (2.1.21). The full Stokes equations take the form as

$$\begin{aligned} -\nu\triangle\boldsymbol{u} + \nabla p &= f, \\ \nabla\cdot\boldsymbol{u} &= 0. \end{aligned} \tag{2.1.22}$$

□

Remark 2.1.9 (Oseen Equation) As a model problem for linearized Navier-Stokes equations, the most general form of the Oseen equation is written as

$$\begin{aligned} -\nu\triangle\boldsymbol{u} + (\boldsymbol{b}\cdot\nabla)\boldsymbol{u} + \nabla p + c\boldsymbol{u} &= f, \\ \nabla\cdot\boldsymbol{u} &= 0, \end{aligned} \tag{2.1.23}$$

where $c \geqslant 0$ and $\boldsymbol{b}$ is a known convection field. □

2.2 Galerkin Discretization with Inf-Sup Stable Pairs of Finite Element Spaces

In the previous section, we derived the Navier-Stokes equations, however, due to the nonlinear terms it contains, the equations are difficult to solve exactly, except under specific conditions. In practical situations, simplification of the equations can be achieved by neglecting certain terms. For instance, when the Reynolds number is small, the inertial forces in the equations can be considered negligible in comparison to the viscous forces, thus reducing the equations to the Stokes equations. The study of the numerical solutions of the Stokes equations not only offers insight into certain aspects of fluid

dynamics, but also serves as a foundation for further research on the Navier-Stokes equations, see [2].
To approximate the numerical solutions of the Stokes equations, the Galerkin finite element method can be employed to discretize the variables of the weak formulation using standard finite element spaces. In this section, we first derive the weak formulation of the Stokes equations, and subsequently apply this formulation to obtain the so-called inf-sup condition, which is utilized to analyze the well-posedness of the Stokes problem. Furthermore, we demonstrate the discrete inf-sup condition within finite element spaces, and derive standard error estimates for the analysis. Finally, a typical family of inf-sup stable finite element spaces is presented.

2.2.1 Weak Formulation and Inf-Sup Condition

Remark 2.2.1 (The Stokes Equations in Weak Form) Consider the Stokes equations with homogenous Dirichlet boundary conditions

$$\begin{aligned} -\nu\triangle \boldsymbol{u} + \nabla p = f \quad &\text{in} \quad \Omega, \\ \nabla \cdot \boldsymbol{u} = 0 \quad &\text{in} \quad \Omega, \\ \boldsymbol{u} = 0 \quad &\text{on} \quad \partial\Omega, \end{aligned} \tag{2.2.1}$$

where $\boldsymbol{u}$ is the velocity field of an incompressible fluid motion, p is the associated pressure. It is obvious that all the solutions to the Stokes equations (2.2.1) should fulfill $\boldsymbol{u} \in C^2(\Omega) \cap C(\bar{\Omega})$ and $p \in C^1(\Omega)$. However, the pressure is not unique since only the pressure gradient enters the equation, not the absolute value of p. Hence, the pressure solution is only unique up to a constant. One can fix this by demanding $\int_\Omega p dx = 0$, define the pressure space consisting of functions with zero mean value on Ω.
Multiplying a test function $\boldsymbol{v} \in H_0^1(\Omega)^d$ and $q \in L_0^2(\Omega)$ in (2.2.1), integrating over Ω, and using integration by parts, we obtain the corresponding weak formulation of the Stokes equations: Find a $(\boldsymbol{u}, p) \in V \times Q$ in a Lipschitz domain with the polyhedral boundary $\Omega \subset R^d$, for all $(\boldsymbol{v}, q) \in V \times Q$ such that

$$\begin{aligned} (\nu\nabla\boldsymbol{u}, \nabla\boldsymbol{v}) - (p, \nabla\cdot\boldsymbol{v}) &= F(\boldsymbol{v}), \\ (\nabla\cdot\boldsymbol{u}, q) &= 0, \end{aligned} \tag{2.2.2}$$

where the operator $F : H^{-1}(\Omega)^d \mapsto \mathbb{R}, F(\boldsymbol{v}) = \langle \boldsymbol{f}, \boldsymbol{v}\rangle = \int_\Omega \boldsymbol{f}\cdot\boldsymbol{v}$, and $V = H_0^1(\Omega)^d$, $Q = L_0^2(\Omega)$. Since it requires $\nabla\boldsymbol{u} \in L^2(\Omega)$, the velocity $\boldsymbol{u}$ should satisfy the Dirichlet boundary condition, and the pressure p has to be unique. The setting for the Stokes equations is:

- Space:

$$V = H_0^1(\Omega)^d \text{ with norm } \|\boldsymbol{v}\|_V = \|\nabla \boldsymbol{v}\|_{L^2(\Omega)},$$
$$Q = L_0^2(\Omega) = \left\{ q : q \in L^2(\Omega), \int_\Omega q dx = 0 \right\} \text{ with norm } \|q\|_{L^2(\Omega)},$$
$$V' = H^{-1} \text{ is the dual space of } V,$$
$$Q' = Q \text{ is the dual spcae of } Q.$$

- Bilinear forms :

$$a(\cdot,\cdot) : V \times V \to R \ , b(\cdot,\cdot) : V \times Q \to R,$$
$$a(\boldsymbol{u},\boldsymbol{v}) = \int_\Omega \nu(\nabla \boldsymbol{u} : \nabla \boldsymbol{v}) d\boldsymbol{x} \text{ ,with norm } \|a\| = \sup_{\boldsymbol{v},\boldsymbol{w} \in V, \boldsymbol{v},\boldsymbol{w} \neq 0} \frac{a(\boldsymbol{v},\boldsymbol{w})}{\|\boldsymbol{v}\|_V \|\boldsymbol{w}\|_Q},$$
$$b(\boldsymbol{v},q) = -\int_\Omega (\nabla \cdot \boldsymbol{v}) q d\boldsymbol{x}, \text{ with norm } \|b\| = \sup_{\boldsymbol{v} \in V, q \in Q, \boldsymbol{v}, q \neq 0} \frac{b(\boldsymbol{v},q)}{\|\boldsymbol{v}\|_V \|q\|_Q}.$$

- Operators :

$$A \in \mathcal{L}(V,V'), \quad A' \in \mathcal{L}(V',V),$$
$$\text{defined by } \langle Au, v \rangle_{V',V} = \langle u, A'v \rangle_{V,V'} = a(u,v) = \nu(\nabla u, \nabla v).$$
$$B \in \mathcal{L}(V,Q'), \quad B' \in \mathcal{L}(Q,V'),$$
$$\text{defined by } \langle Bv, q \rangle_{Q',Q} = \langle v, B'q \rangle_{V,V'} = b(v,q) = (\nabla \cdot v, q).$$

Two continuous bilinear form $a(\cdot,\cdot)$ and $b(\cdot,\cdot)$ mentioned above are bounded,

$$a(\boldsymbol{u},\boldsymbol{v}) \leqslant C_1 \|\boldsymbol{u}\|_V \|\boldsymbol{v}\|_V, \tag{2.2.3}$$

$$b(\boldsymbol{v},\boldsymbol{q}) \leqslant C_2 \|\boldsymbol{v}\|_V \|\boldsymbol{q}\|_Q, \tag{2.2.4}$$

for all $\boldsymbol{u},\boldsymbol{v} \in V$ and $q \in Q$.
Using the bilinear form, the weak formulation (2.2.2) can be written as

$$\begin{aligned} a(\boldsymbol{u},\boldsymbol{v}) + b(\boldsymbol{v},p) &= F(\boldsymbol{v}), \\ b(\boldsymbol{u},q) &= 0. \end{aligned} \tag{2.2.5}$$

With the introduced operators, the weak formulation (2.2.2) also has an equivalent form as follows:

$$\begin{aligned} A\boldsymbol{u} + B'p &= f, \\ B\boldsymbol{u} &= 0. \end{aligned} \tag{2.2.6}$$

□

Remark 2.2.2 In order to investigate whether there is a unique solution $(\boldsymbol{u}, p)$ to the Stokes equations (2.2.1), we first restrict ourselves to a divergence-free velocity space to consider the velocity $\boldsymbol{u}$ and then prove that there exists a corresponding pressure p satisfying the Stokes equations (2.2.1). $\square$

Lemma 2.2.1 Let Φ be an linear operator, from $V \times Q$ onto $V' \times Q'$,

$$\Phi(\boldsymbol{v}, q) = (A\boldsymbol{v} + B'q, B\boldsymbol{v}).$$

Thus, (2.2.6) is called well-posedness if Φ is an isomorphism. $\square$

Remark 2.2.3 (Divergence-Free Space) For incompressible flow problems, the mass conservation property is described by

$$\int_\Omega \nabla \cdot \boldsymbol{u} q dx = 0, \quad \forall q \in L_0^2(\Omega), \tag{2.2.7}$$

in the weak formulation. Hence, $\nabla \cdot \boldsymbol{u} = 0$ holds on Ω in L^2 sense. Then, the space of vector fields in $L^2(\Omega)$ where the divergence also belongs to $L^2(\Omega)$, is defined as

$$H(\text{div}, \Omega) = \{\boldsymbol{v} \in L^2(\Omega) : \ \nabla \cdot \boldsymbol{v} \in L^2(\Omega)\}.$$

A particular space of divergence-free functions is defined by

$$\begin{aligned} H_{div,\Omega} = \{\boldsymbol{v} \in H(\text{div}, \Omega) : \nabla \cdot \boldsymbol{v} = 0 \text{ and } \boldsymbol{v} \cdot \boldsymbol{n} = 0 \text{ on } \partial\Omega \\ \text{in the sense of traces}\}. \end{aligned}$$

The function $\psi \in L^1_{loc}(\Omega)$ is called the weak divergence of $\boldsymbol{v} \in L^p(\Omega)$ such that

$$\int_\Omega \psi \phi dx = -\int_\Omega \nabla \phi \cdot \boldsymbol{v} dx, \ \forall \phi \in C_0^\infty(\Omega).$$

Then, the vector field $\boldsymbol{v} \in L^p(\Omega)$ is called weakly divergence-free if

$$\int_\Omega \nabla \phi \cdot \boldsymbol{v} dx = 0, \ \forall \phi \in C_0^\infty(\Omega).$$

Using the above operator, the space of weakly divergence-free functions is defined as follows, $\forall \boldsymbol{v} \in H_0^1(\Omega)^d$,

$$\begin{aligned} V^{div} &: = \{b(\boldsymbol{v}, q) = 0, \forall q \in L_0^2(\Omega)\}, \\ &= \{B\boldsymbol{v} = 0\} = Ker(B), \end{aligned}$$

where the $Ker(B)$ is the kernel of operator B .
The orthogonal complement of V^{div} in $H_0^1(\Omega)^d$ is denoted as

$$V^{div,\perp} := \{\boldsymbol{w} \in H_0^1(\Omega)^d, a(\boldsymbol{v}, \boldsymbol{w}) = 0, \forall \boldsymbol{v} \in V^{div}\}. \tag{2.2.8}$$

$\square$

Lemma 2.2.2 V^{div} is a linear, closed subspace of V, it is also a Hilbert space.

Proof: By the definition of V^{div}, it is a subset of V.
Since $\mathbf{0} \in V^{div}$, $V^{div} \neq \varnothing$. Consider any two vectors $\boldsymbol{v}$, $\boldsymbol{w} \in V^{div}$, and any two scalars $\alpha, \beta \in \mathbb{R}$, then the linear combination

$$\begin{aligned} b(\alpha\boldsymbol{v} + \beta\boldsymbol{w}) &= -\int_\Omega \nabla \cdot (\alpha\boldsymbol{v} + \beta\boldsymbol{w}) q dx \\ &= -\alpha \int_\Omega (\nabla \cdot \boldsymbol{v}) q dx - \beta \int_\Omega (\nabla \cdot \boldsymbol{w}) q dx \\ &= \alpha b(\boldsymbol{v}, q) + \beta b(\boldsymbol{w}, q) = 0, \end{aligned} \tag{2.2.9}$$

also belongs to the space V^{div}. Thus, the space V^{div} is linear.
Let $\{\boldsymbol{v_n}\}_{n=1}^{\infty}$ be an arbitrary Cauchy sequence with $\boldsymbol{v_n} \in V^{div}$. Since V is complete, there exists a $\boldsymbol{v} \in V$, such that $\lim_{n\to\infty} \boldsymbol{v_n} = \boldsymbol{v}$. To show the closeness of V^{div}, one has to show that $\boldsymbol{v} \in V^{div}$. By the continuity of the bilinear form $b(\cdot, \cdot)$, we have

$$b(\boldsymbol{v}, q) = b(\lim_{n\to\infty} \boldsymbol{v_n}, q) = \lim_{n\to\infty} b(\boldsymbol{v_n}, q) = 0. \tag{2.2.10}$$

Hence, $\boldsymbol{v} \in V^{div}$.
As a linear, closed subspace of a Hilbert space is a Hilbert space itself, thus, V^{div} is a Hilbert space. ∎

Theorem 2.2.1 (Lax-Milgram Theorem) For a bilinear form $a(\cdot, \cdot)$ on $V \times V$, if it satisfies

1) Continuity: $a(\boldsymbol{u}, \boldsymbol{v}) \leqslant \beta \|\boldsymbol{u}\|_V \|\boldsymbol{v}\|_V$, $\beta \in \mathbb{R}$,
2) Coercivity : $a(\boldsymbol{u}, \boldsymbol{u}) \geqslant \alpha \|\boldsymbol{u}\|_V^2$, $\alpha > 0$,

then for any $f \in V'$, there exists a unique $\boldsymbol{u} \in V$ such that

$$a(\boldsymbol{u}, \boldsymbol{v}) = \langle f, \boldsymbol{v} \rangle, \tag{2.2.11}$$

and

$$\|\boldsymbol{u}\|_V \leqslant \frac{1}{\alpha} \|f\|_{V'}. \tag{2.2.12}$$

Proof: Applying the Riesz Representation Theorem, the existence and uniqueness of $\boldsymbol{u} \in V$ satisfying (2.2.11) can be proved in [3] on pages 315 and 316. For (2.2.12), we have

$$\alpha \|\boldsymbol{u}\|_V^2 \leqslant a(\boldsymbol{u}, \boldsymbol{u}) = \langle f, \boldsymbol{u} \rangle \leqslant \|f\|_{V'} \|\boldsymbol{u}\|_V,$$

which completes the proof of the Lax-Milgram Theorem.

∎

Remark 2.2.4 For (2.2.5), we remove the pressure term and consider only the velocity $\boldsymbol{u} \in V^{div}$. For a given $f \in H^{-1}(\Omega)$, find $\boldsymbol{u} \in V^{div}$ such that

$$a(\boldsymbol{u}, \boldsymbol{v}) = \langle f, \boldsymbol{v} \rangle, \forall \boldsymbol{v} \in V^{div}. \tag{2.2.13}$$

Since V^{div} is a Hilbert space with the inner product, the bilinear form $a(\cdot, \cdot)$ is bounded and coercive which fulfills the conditions in the Lax-Milgram theorem. Thus, there exists a unique solution to (2.2.13). The remaining question about the well-posedness of (2.2.5) is whether there exists a unique p such that $(\boldsymbol{u}, p)$ is a solution to (2.2.5) when $\boldsymbol{u} \in V^{div}$ solving (2.2.13) exists.
Assume $\boldsymbol{u} \in V^{div}$ is the solution to (2.2.13), the first equation of (2.2.5) can be written as

$$b(\boldsymbol{v}, p) = -a(\boldsymbol{u}, \boldsymbol{v}) + F(\boldsymbol{v}), \quad \forall \boldsymbol{v} \in V. \tag{2.2.14}$$

Problem (2.2.14) also has the following form,

$$b(\boldsymbol{v}, p) = \tilde{F}(\boldsymbol{v}), \quad \forall \boldsymbol{v} \in V, \tag{2.2.15}$$

where $\tilde{F}(\boldsymbol{v}) = 0$, for all $\boldsymbol{v} \in V^{div}$.
The Lax-Milgram theorem cannot be applied to prove the existence problem of the solution to this equation, because the bilinear form $b(\cdot, \cdot)$ is not coercive. Therefore, we introduce the equivalent condition to solve this problem, namely the inf-sup condition. □

Definition 2.2.1 (Inf-Sup Condition) Consider the bilinear form $b(\cdot, \cdot) : V \times Q \to \mathbb{R}$, if there exists a constant $\beta > 0$ such that

$$\inf_{q \in Q \backslash \{0\}} \sup_{\boldsymbol{v} \in V \backslash \{0\}} \frac{b(\boldsymbol{v}, q)}{\|\boldsymbol{v}\|_V \|q\|_Q} \geqslant \beta > 0, \tag{2.2.16}$$

then this is the so-called inf-sup condition. □

Remark 2.2.5 The equation (2.2.16) can be written as that for all $q \in Q$

$$\beta \|q\|_Q \leqslant \sup_{\boldsymbol{v} \in V \backslash \{0\}} \frac{b(\boldsymbol{v}, q)}{\|\boldsymbol{v}\|_V},$$

this inequality relates to the coercivity condition (2.2.4),

$$\alpha \|\boldsymbol{u}\|_V \leqslant \sup_{\boldsymbol{u} \in V \backslash \{0\}} \frac{a(\boldsymbol{u}, \boldsymbol{u})}{\|\boldsymbol{u}\|_V} \leqslant \sup_{\boldsymbol{v} \in V \backslash \{0\}} \frac{a(\boldsymbol{v}, \boldsymbol{u})}{\|\boldsymbol{v}\|_V}.$$

The inf-sup condition (2.2.16) can be regarded as a new coercivity condition for (2.2.14).

Lemma 2.2.3 The following properties are equivalent:

(i) There exist a constant $\beta > 0$ such that

$$\inf_{q \in Q \setminus \{0\}} \sup_{\boldsymbol{v} \in V \setminus \{0\}} \frac{b(\boldsymbol{v}, q)}{\|\boldsymbol{v}\|_V \|q\|_Q} \geqslant \beta > 0. \tag{2.2.17}$$

(ii) The operator B' is an isomorphism from Q onto $\tilde{V}'$ and

$$\|B'q\|_{V'} \geqslant \beta \|q\|_Q, \;\; \forall q \in Q \tag{2.2.18}$$

where $\tilde{V}' := \{g \in V', \langle g, \boldsymbol{v} \rangle_{V',V} = 0, \forall \boldsymbol{v} \in V^{div}\}$.

(iii) The operator B is an isomorphism from $V^{div,\perp}$ onto Q' and

$$\|B\boldsymbol{v}\|_{Q'} \geqslant \beta \|\boldsymbol{v}\|_V, \;\; \forall \boldsymbol{v} \in V^{div,\perp}. \tag{2.2.19}$$

Proof: See [4] on pages 58 and 59. ■

Definition 2.2.2 Define a linear continuous operator $\Pi \in \mathcal{L}(V', (V^{div})')$ by:

$$\langle \Pi f, \boldsymbol{v} \rangle_{V',V} = \langle f, \boldsymbol{v} \rangle_{V',V}, \quad \forall f \in V', \forall \boldsymbol{v} \in V^{div}. \tag{2.2.20}$$

This operator Πf restrict f from V' onto $(V^{div})'$. With this operator, we complete the conditions for satisfying the well-posedness of the Stokes problem (2.2.6). □

Theorem 2.2.2 (Well-posedness of the Stokes Problem (2.2.6)**)** Problem (2.2.6) is well-posed (i.e., the operator Φ is isomorphism) if and only if the following conditions hold:

(1) the operator ΠA is an isomorphism from V to V',

(2) the bilinear form $b(\cdot, \cdot)$ satisfies the inf-sup condition (2.2.16).

Proof: See [4], page 59. ■

Corollary 2.2.1 Assume that the bilinear form $b(\cdot, \cdot)$ is V-elliptic, i.e., there exists a constant $\alpha > 0$ such that

$$a(\boldsymbol{v}, \boldsymbol{v}) \geqslant \alpha \|\boldsymbol{v}\|_V^2.$$

Then, the problem (2.2.6) is well-posed if and only if the bilinear form $b(\cdot, \cdot)$ satisfies the inf-sup condition (2.2.16).

Proof: See [4], page 61. ■

2.2.2 Finite Element Space and the Discrete Inf-Sup Condition

The uniqueness and existence of solutions to the Stokes equations were proved in the previous section. The next step is to find approximate solutions since the function spaces V and Q are in infinite dimensions, making numerical computation intractable. Then, a better-suited finite element space will be introduced.

Remark 2.2.6 (Finite Element) A finite element can be defined as a triple $\{K, \mathcal{P}, \mathcal{N}\}$ which consists of

- K is a bounded closed set of $\mathbb{R}^n$ with nonempty interior and piecewise smooth boundary.
- $\mathcal{P}$ is the finite-dimensional space that consists of polynomials defined on K.
- $\mathcal{N} = \{N_1, N_2, ..., N_k\}$ is the set of nodal variables which forms the basis for the space $\mathcal{P}'$.

□

Definition 2.2.3 (Unisolvence) The space $\mathcal{P}$ is called unisolvent with respect to functionals $\mathcal{N}$ if for each $\boldsymbol{a} = (a_1, .., a_k) \in \mathbb{R}^k$, there is exact one $p \in \mathcal{P}$ such that

$$N_i(p) = a_i. \tag{2.2.21}$$

□

Definition 2.2.4 (Local Nodal Basis) By the meaning of unisolvence, there exists a set of $\{\phi_k\}_{i=1}^k$ such that

$$N_i(\phi_j) = \delta_{ij}, \tag{2.2.22}$$

which is called local nodal basis. □

Definition 2.2.5 (Triangulation) Let $\mathcal{T}_h$ be a triangulation of Ω. The domain is subdivided into a finite number of subsets K in such a way that:

- $\overline{\Omega} = \bigcup_{K \in \mathcal{T}_h} K$.
- Each $K \in \mathcal{T}_h$ is a closed polyhedron and $\mathring{K}$ is nonempty.
- For any two elements K_1, K_2 we have either $K_1 = K_2$ or $\mathring{K}_1 = \mathring{K}_2 = \varnothing$.

- If $e = K_1 \cap K_2 \neq \varnothing$, then e is either a common face, edge, or vertex of K_1 and K_2.

- For every $K \in \mathcal{T}_h$, the boundary ∂K is Lipschitz continuous.

$\square$

Definition 2.2.6 (Finite Element Space, Global Basis) In order to uniquely determine a finite element space, continuity requirements between mesh cells must be specified as follows: the function v defined on finite element space Ω with $v\ |_K \in \mathcal{P}$ for all $K \in \mathcal{T}_h$ is called continuous with respect to the functional $N_i \in \mathcal{N} : \Omega \mapsto \mathbb{R}$ if

$$N_i(v\ |_{K_1}) = N_i(v\ |_{K_2}),\ \forall K_1, K_2 \in w_i, \tag{2.2.23}$$

where w_i is the union of all mesh cells K_j, for which there is a $p \in \mathcal{P}(K_j)$ with $N_i(p) \neq 0$.
The space

$$S = \{v \in L^\infty(\Omega) : v\ |_K \in \mathcal{P} \text{ and } v \text{ is continuous with respect to } N_i, i = 1, ..., k\},$$

is called the finite element space.
The global basis $\{\phi_i\}_{i=1}^k$ of S is defined by the condition

$$\phi_i \in S,\ N_j(\phi_i) = \delta_{ij},\ i, j = 1, ..., k.$$

In each cell, a global basis function coincides with a local basis function, which implies the uniqueness of the global basis function.
The continuity of the finite element functions is not always guaranteed by the continuity of the global functionals $\{N_i\}_{i=1}^k$, as it is determined by the definition of the functionals defining the finite element space. $\square$

Remark 2.2.7 (Piecewise Polynomial Spaces) Let $\mathcal{P}_K$ be the set of all polynomials whose degree is less than or equal to k with variables $x_1, ..., x_d$. Then, for any $p \in \mathcal{P}_K$ is defined as following:

$$p(x_1, x_2, ..., x_d) = \sum C_{\boldsymbol{\alpha}} x_1^{\alpha_1} x_2^{\alpha_2} ... x_d^{\alpha_d}, \quad \alpha_1 + ... + \alpha_d \leqslant k, \tag{2.2.24}$$

where $\boldsymbol{\alpha} = (\alpha_1, ..., \alpha_d)$. Thus the number of different terms is the same as the number of choosing k elements from the set $\{1, x_1, ..., x + d\}$ with repetition allowed. Thus

$$dim \mathcal{P}_k = \binom{d+k}{k}. \tag{2.2.25}$$

The functional variables $N_k \in \mathcal{N}$ that uniquely determine the function in the space $\mathcal{P}_K$ are called the degrees of freedom, and we often use $\sum_K$ to denote the set of the degrees of freedom. $\square$

Definition 2.2.7 (The Finite Element Discretization of the Stokes Equations) Finite element methods for solving the Stokes equation can be viewed as a specific application of the Galerkin method. This involves choosing subspaces $V_h \subset V$ and $Q_h \subset Q$ based on a triangulation $\mathcal{T}_h$ of the domain Ω, and considering the variational problem (2.2.5) in a finite-dimensional setting. Specifically, the goal is to find $(\boldsymbol{u}_h, p_h) \in V_h \times Q_h$ such that for all $(\boldsymbol{v}_h, q_h) \in V_h \times Q_h$:

$$\begin{aligned} a_h(\boldsymbol{u}_h, \boldsymbol{v}_h) + b_h(p_h, \boldsymbol{v}_h) &= F(\boldsymbol{v}_h), \\ b_h(\boldsymbol{u}_h, q_h) &= 0, \end{aligned} \tag{2.2.26}$$

with bilinear forms:

$$\begin{aligned} a_h : V_h \times V_h \mapsto \mathbb{R},\ a_h(\boldsymbol{u}_h, \boldsymbol{v}_h) &= \sum_{K \in \mathcal{T}_h} \nu(\nabla \boldsymbol{u}_h, \nabla \boldsymbol{v}_h)_K, \\ b_h : V_h \times Q_h \mapsto \mathbb{R},\ b_h(\boldsymbol{v}_h, q_h) &= -\sum_{K \in \mathcal{T}_h} (\nabla \boldsymbol{v}_h, q_h)_K. \end{aligned}$$

□

Remark 2.2.8 Regarding the existence and uniqueness of solutions to the Stokes problem, Theorem 2.2.2 and Corollary 2.2.1 state that the variational problem (2.2.5) needs to satisfy the requirement that bilinear form $a(\cdot, \cdot)$ is coercive and $b(\cdot, \cdot)$ fulfills the inf-sup condition (2.2.16). Similarly, the same conditions should be satisfied for the discrete problem (2.2.26). Since the subspace $V_h \subset V$ and $Q_h \subset Q$, the bilinear form $b_h(\cdot, \cdot)$ is identical to the bilinaer form $b(\cdot, \cdot)$. □

Theorem 2.2.3 (The Discrete Inf-Sup Condition) The discrete inf-sup condition for the finite element approximation is defined as follows:

$$\inf_{q_h \in Q_h \backslash \{0\}} \sup_{\boldsymbol{v_h} \in V_h \backslash \{0\}} \frac{b(\boldsymbol{v_h}, q_h)}{\|\boldsymbol{v_h}\|_{V_h} \|q_h\|_{Q_h}} = \beta_h > 0. \tag{2.2.27}$$

□

Remark 2.2.9 If the bilinear form $a_h(\cdot, \cdot)$ is V_h-elliptic, and the bilinear form $b_h(\cdot, \cdot)$ satisfies the discrete inf-sup condition (2.2.27), the finite element Stokes equations (2.2.26) has a unique solution. □

2.2.3 Galerkin Finite Element Method and Standard Error Analysis

Remark 2.2.10 (Galerkin Discretization of the Stokes Problem) Consider a finite-dimensional subspace V_h and Q_h, let

$$
\begin{aligned}
V_h &= \operatorname{span}\{\boldsymbol{\phi}_j\}_{j=1}^{3N} \\
&= \operatorname{span}\left\{ \left\{\begin{pmatrix}\phi_j\\0\\0\end{pmatrix}\right\}_{j=1}^{N} \cup \left\{\begin{pmatrix}0\\\phi_j\\0\end{pmatrix}\right\}_{j=1}^{N} \cup \left\{\begin{pmatrix}0\\0\\\phi_j\end{pmatrix}\right\}_{j=1}^{N} \right\},
\end{aligned}
$$

be the basis of the vector-valued velocity space. Each basis function has non-zero coefficients in more than one component.
Let $\{\psi\}_{i=1}^{M}$ be the basis of the pressure finite element spaces Q_h. Hence, $\dim(V_h) = 3N, \dim(Q_h) = M$. Then, for any function $\boldsymbol{u}_h \in V_h$ and $p_h \in Q_h$ there is a unique representation:

$$
\begin{aligned}
\boldsymbol{u}_h &= \sum_{j=1}^{3N} \alpha_j \boldsymbol{\phi}_j, \\
p_h &= \sum_{k=1}^{M} \beta_k \psi_k.
\end{aligned}
\tag{2.2.28}
$$

Then, taking them to the finite-dimensional variational problem (2.2.26) to get

$$
\begin{aligned}
\sum_{j=1}^{3N} a(\boldsymbol{\phi_j}, \boldsymbol{\phi_i})\alpha_j + \sum_{k=1}^{M} b(\boldsymbol{\phi}_i, \psi_k)\beta_k &= (f_h, \boldsymbol{\phi}_i), \qquad i = 1, 2, ..., 3N, \\
\sum_{j=1}^{3N} b(\boldsymbol{\phi}_j, \psi_i)\alpha_j &= 0, \qquad i = 1, 2, ..., M.
\end{aligned}
\tag{2.2.29}
$$

It reveals that the Galerkin method transforms the problem of solving partial differential equations into finding the coefficient vector $\{\alpha_j\}_{1=0}^{3N}$ and $\{\beta_k\}_{k=1}^{M}$ so that the (2.2.29) is satisfied.

By introducing

$$A_h = (a_{ij})_{N\times N} \text{ with } a_{ij} := a(\boldsymbol{\phi}_j, \boldsymbol{\phi_i}) = \sum_{K\in\mathcal{T}_h} \nu(\nabla\boldsymbol{\phi}_j, \nabla\boldsymbol{\phi}_i)_K,$$
$$B_h = (b_{ij})_{M\times N} \text{ with } b_{ij} := b(\boldsymbol{\phi}_j, \psi_i) = -\sum_{K\in\mathcal{T}_h} (\nabla\boldsymbol{\phi}_j, \nabla\psi_i)_K,$$
$$(\underline{f})_i = f_i = \sum_{K\in\mathcal{T}_h} (f_h, \boldsymbol{\phi}_i), \ \underline{f} \in \mathbb{R}^{3N},$$
$$(\underline{u})_j = \alpha_j, \ \underline{u} \in \mathbb{R}^{3N}, \ (\underline{p})_k = \beta_k, \ \underline{p} \in \mathbb{R}^M,$$

the coefficient vector can be obtained by solving the following linear system of block matrix form as follows

$$\begin{pmatrix} A_h & B_h^T \\ B_h & 0 \end{pmatrix} \begin{pmatrix} \underline{u} \\ \underline{p} \end{pmatrix} = \begin{pmatrix} \underline{f} \\ 0 \end{pmatrix}. \tag{2.2.30}$$

□

Remark 2.2.11 The previous section shows $a_h(\cdot,\cdot)$ is coercive and $b_h(\cdot,\cdot)$ satisfies the discrete inf-sup condition, thereby proving the existence and uniqueness of solutions for the discrete Stokes equation. □

Definition 2.2.8 The A_h block represents the contributions of velocity with the momentum equations' test functions. They have interactions of $\nabla\boldsymbol{\phi}_j$ with $\nabla\boldsymbol{\phi}_i$ only if $i = j$. Thus, the A_h is a block-diagonal matrix. Moreover, the non-zero components of $\nabla\boldsymbol{\phi}_j$ with $\nabla\boldsymbol{\phi}_i$ have the same value. Hence, the matrix A_h has the structure

$$A_h = \begin{pmatrix} A_{11} & 0 & 0 \\ 0 & A_{11} & 0 \\ 0 & 0 & A_{11} \end{pmatrix}. \tag{2.2.31}$$

□

Lemma 2.2.4 (Properties of the Matrix A_h) A_h is symmetric and positive definite.

Proof: From the definition of A_h, it is easy to prove the symmetry.
In order to prove the positive definiteness, one can choose an arbitrary $\boldsymbol{v}_h \in$

V_h with $\boldsymbol{v}_h \neq \mathbf{0}$ which is defined as $\boldsymbol{v}_h = \sum_{j=1}^{3N} v_j \boldsymbol{\phi}_j$ with $\underline{v}_h \in \mathbb{R}^{3N} \backslash \{\underline{0}\}$, then

$$\begin{aligned}
\underline{v}_h^T A_h \underline{v}_h &= \sum_{i,j=1}^{3N} v_j v_i \sum_{K \in \mathcal{T}_h} \nu(\nabla \boldsymbol{\phi}_j, \nabla \boldsymbol{\phi}_i)_K \\
&= \sum_{K \in \mathcal{T}_h} \nu(\sum_{i,j=1}^{3N} v_j \nabla \boldsymbol{\phi}_j, \sum_{i,j=1}^{3N} v_i \nabla \boldsymbol{\phi}_i)_K \\
&= \sum_{K \in \mathcal{T}_h} \nu(\nabla \boldsymbol{v}_h, \nabla \boldsymbol{v}_h) \\
&= a(\boldsymbol{v}_h, \boldsymbol{v}_h) \\
&= \|\boldsymbol{v}_h\|_{V_h}^2 > 0.
\end{aligned}$$

■

Lemma 2.2.5 (Properties of the Matrix B_h) The discrete inf-sup condition (2.2.27) implies that the matrix B_h has full rank and $\dim(V_h) \geqslant \dim(Q_h)$.

Proof: The matrix $B_h \in \mathbb{R}^{M \times 3N}$ is defined as

$$(B_h)_{ij} = b(\boldsymbol{\phi}_j, \psi_i).$$

From the discrete inf-sup condition (2.2.27), it follows that for every $\psi_h \in Q_h, \psi_h \neq 0$, there exists $\boldsymbol{\phi}_h \in V_h$ such that $b(\boldsymbol{\phi}_h, \psi_h) \neq 0$. Thus for every $\underline{y} \in \mathbb{R}^M, \underline{y} \neq 0$, there exists $\underline{x} \in \mathbb{R}^{3N}$ such that $\underline{y}^T B_h \underline{x} \neq 0$, and also $\underline{x}^T B_h^T \underline{y} \neq 0$. This means that all columns of B_h^T and all rows of B_h are independent. A necessary condition for this is $M \leqslant 3N$. ■

Remark 2.2.12 Lemmas 2.2.4 and 2.2.5 guarantee the solvability of the linear equation system described in (2.2.30). The application of the Galerkin finite element method to solve the Stokes equations is complicated by the coupling of pressure and velocity spaces. Lemma 2.2.5 provides guidance on suitable choices for finite element spaces, based on the discrete inf-sup condition, indicating that the velocity space V_h should be larger than the pressure space Q_h.
To analyze the errors in the velocity and pressure solutions of the Stokes equations, a discrete divergence-free space can be introduced. □

Remark 2.2.13 (Discrete Divergence-Free Space) In the discrete problem, with the finite element spaces V_h and Q_h for velocity and pressure respectively, one obtains the variational equation

$$\int_\Omega \nabla \cdot \boldsymbol{u}_h q_h dx = 0, \quad \forall q_h \in Q_h, \tag{2.2.32}$$

where the discrete velocity solution $\boldsymbol{u}_h \in V_h$, such $\boldsymbol{u}_h$ is called discretely divergence-free. The space V_h^{div} of discretely divergence-free functions is defined as follows:

$$V_h^{div} = \{\boldsymbol{v}_h \in V_h \ : \ b(\boldsymbol{v}_h, q_h) = 0, \quad \forall q_h \in Q_h\}, \tag{2.2.33}$$

which is the kernel of B_h. The operator B_h maps from V_h to Q_h, such that $(B_h \boldsymbol{v}_h, q_h) = b(\boldsymbol{v}_h, q_h)$. Usually this does not imply $\nabla \cdot \boldsymbol{u}_h = 0$ in Ω due to $Q_h \neq L_0^2(\Omega)$. It means a discrete divergence-free function may not be exactly divergence-free, i.e., $V_h^{div} \not\subset V^{div}$. This will lead to the violation of mass conservation which we have to be aware of in finite element discretization. ▫

Theorem 2.2.4 (Error Estimate for the Gradient of Velocity) Let $(\boldsymbol{u}, p)$ be the unique solution of the Stokes equation (2.2.5). This problem is discretized to (2.2.26) using the inf-sup stable finite element space $V_h \times Q_h \subset V \times Q$, with the velocity solution represented by $\boldsymbol{u}_h \in V_h^{div}$. Then, the following error estimate holds

$$\|\nabla(\boldsymbol{u} - \boldsymbol{u}_h)\|_{L^2(\Omega)} \leqslant 2 \inf_{\boldsymbol{v}_h \in V_h^{div}} \|\nabla(\boldsymbol{u} - \boldsymbol{v}_h)\|_{L^2(\Omega)} + \nu^{-1} \inf_{q_h \in Q_h} \|p - q_h\|_{L^2(\Omega)}. \tag{2.2.34}$$

Proof: Firstly, one needs to choose a proper test function to formulate weak equations. With the property in Remark 2.2.13, the discretely divergence-free functions from $V_h^{div} \in V$ can be used in both original (2.2.5) and discrete (2.2.26) problem, then subtract one from the other to obtain

$$a(\boldsymbol{u} - \boldsymbol{u}_h, \boldsymbol{v}_h) + b(\boldsymbol{v}_h, p) = 0, \ \forall \boldsymbol{v}_h \in V_h^{div}, \tag{2.2.35}$$

due to the discretely divergence free $b(\boldsymbol{v}_h, p_h) = 0$. Moreover, the pressure term cannot be removed from the equation since $V_h^{div} \not\subset V^{div}$. Then, add the term $b(\boldsymbol{v}_h, q_h)$ to the left-hand side of the equation, and the error estimate is reduced to

$$a(\boldsymbol{u} - \boldsymbol{u}_h, \boldsymbol{v}_h) + b(\boldsymbol{v}_h, p - q_h) = 0, \ \forall \boldsymbol{v}_h \in V_h^{div}. \tag{2.2.36}$$

For arbitrary $\boldsymbol{v}_h \in V_h^{div}$, the error is decomposed into

$$\boldsymbol{u} - \boldsymbol{u}_h = (\boldsymbol{u} - \boldsymbol{v}_h) - (\boldsymbol{u}_h - \boldsymbol{v}_h) := \boldsymbol{\eta} - \boldsymbol{\phi}_h.$$

Since $\boldsymbol{\phi}_h \in V_h^{div}$, it can be used as a test function that takes the place of $\boldsymbol{v}_h$. Thus, by taking the error decomposition and using the test function $\boldsymbol{v}_h = \boldsymbol{\phi}_h$ in (2.2.36), one obtains

$$\nu \|\nabla \boldsymbol{\phi}_h\|_{L^2(\Omega)}^2 = \nu(\nabla \boldsymbol{\eta}, \nabla \boldsymbol{\phi}_h) - (\nabla \cdot \boldsymbol{\phi}_h, p - q_h). \tag{2.2.37}$$

Using the Cauchy-Schwarz inequality to the first term and the second term on the right-hand side, yields

$$\begin{aligned}\nu\|\nabla\boldsymbol{\phi}_h\|^2_{L^2(\Omega)} \leqslant \nu\|\nabla\boldsymbol{\eta}\|_{L^2(\Omega)}\|\nabla\boldsymbol{\phi_h}\|_{L^2(\Omega)} \\ + \|\nabla\cdot\boldsymbol{\phi}_h\|_{L^2(\Omega)}\|(p-q_h)\|_{L^2(\Omega)}.\end{aligned} \tag{2.2.38}$$

Applying the divergence estimate $\|\nabla\cdot\boldsymbol{\phi}_h\|_{L^2(\Omega)} \leqslant \|\nabla\boldsymbol{\phi}_h\|_{L^2(\Omega)}$ by the gradient of functions from $H^1_0(\Omega)$, see [5], then (2.2.37) is divided by $\nu\|\boldsymbol{\phi}_h\|_{L^2(\Omega)} \neq 0$ which leads to

$$\|\nabla\boldsymbol{\phi}_h\|_{L^2(\Omega)} \leqslant \|\nabla\boldsymbol{\eta}\|_{L^2(\Omega)} + \nu^{-1}\|(p-q_h)\|_{L^2(\Omega)}. \tag{2.2.39}$$

This estimate trivially holds if $\|\nabla\boldsymbol{\phi}_h\|_{L^2(\Omega)} = 0$. With the triangle inequality of the gradient of the error decomposition, it gives

$$\begin{aligned}\|\nabla(\boldsymbol{u}-\boldsymbol{u}_h)\|_{L^2(\Omega)} &\leqslant \|\nabla\boldsymbol{\phi}_h\|_{L^2(\Omega)} + \|\nabla\boldsymbol{\eta}\|_{L^2(\Omega)} \\ &\leqslant 2\|\nabla\boldsymbol{\eta}\|_{L^2(\Omega)} + \nu^{-1}\|(p-q_h)\|_{L^2(\Omega)}.\end{aligned}$$

The resulting estimate in terms of the best approximation errors is obtained in (2.2.34). ■

Remark 2.2.14 The error estimate (2.2.34) shows that the velocity error $\|\nabla(\boldsymbol{u}-\boldsymbol{u}_h)\|_{L^2(\Omega)}$ is bounded by the best approximation error of pressure, which is scaled with the inverse of the viscosity. The error estimate would be large if the viscosity is small. □

Corollary 2.2.2 (Error Estimate for the Divergence of Velocity) From (2.2.34), one obtains

$$\|\nabla\cdot\boldsymbol{u}_h\|_{L^2(\Omega)} \leqslant 2\inf_{\boldsymbol{v}_h\in V_h^{div}}\|\nabla(\boldsymbol{u}-\boldsymbol{v}_h)\|_{L^2(\Omega)} + \nu^{-1}\inf_{q_h\in Q_h}\|p-q_h\|_{L^2(\Omega)}. \tag{2.2.40}$$

Proof: Combining with the $\nabla\cdot\boldsymbol{u} = 0$ and the divergence estimate by the gradient, gives

$$\|\nabla\cdot\boldsymbol{u}_h\|_{L^2(\Omega)} = \|\nabla\cdot(\boldsymbol{u}-\boldsymbol{u_h})\|_{L^2(\Omega)} \leqslant \|\nabla(\boldsymbol{u}-\boldsymbol{u}_h)\|_{L^2(\Omega)}.$$

Thus the estimate in (2.2.40) is obtained. ■

Theorem 2.2.5 (Error Estimate of Pressure) The finite element error estimate for the L_2 norm of the pressure is

$$\begin{aligned}\|p-p_h\|_{L^2(\Omega)} \leqslant \frac{2\nu}{\beta_h}\inf_{\boldsymbol{v}_h\in V_h^{div}\setminus\{\boldsymbol{0}\}}\|\nabla\cdot(\boldsymbol{u}-\boldsymbol{v}_h)\|_{L^2(\Omega)} + \\ \left(1+\frac{2}{\beta_h}\right)\inf_{q\in Q_h\setminus\{\boldsymbol{0}\}}\|p-q_h\|_{L^2(\Omega)}.\end{aligned} \tag{2.2.41}$$

Proof: Choosing the test function $(\boldsymbol{v}_h, q_h) \in V_h \times Q_h$, one gets the following with the triangle inequality

$$\|p - p_h\|_{L^2(\Omega)} \leqslant \|p - q_h\|_{L^2(\Omega)} + \|p_h - q_h\|_{L^2(\Omega)}. \tag{2.2.42}$$

By subtracting the first equations in each of Stokes equations (2.2.5) and discrete problem (2.2.26), one finds the relation

$$a(\boldsymbol{u} - \boldsymbol{u}_h, \boldsymbol{v}_h) = b(\boldsymbol{v}_h, p - p_h). \tag{2.2.43}$$

With the inf-sup condition and the Cauchy-Schwarz inequality, one gets

$$\begin{aligned}
&\|p_h - q_h\|_{L^2(\Omega)} \\
&\leqslant \frac{1}{\beta_h} \sup_{\boldsymbol{v}_h \in V_h \setminus \{\mathbf{0}\}} \frac{b(\boldsymbol{v}_h, p_h - q_h)}{\|\nabla \boldsymbol{v}_h\|_{L^2(\Omega)}} \\
&= \frac{1}{\beta_h} \sup_{\boldsymbol{v}_h \in V_h \setminus \{\mathbf{0}\}} \frac{b(\boldsymbol{v}_h, p_h - p) + b(\boldsymbol{v}_h, p - q_h)}{\|\nabla \boldsymbol{v}_h\|_{L^2(\Omega)}} \\
&= \frac{1}{\beta_h} \sup_{\boldsymbol{v}_h \in V_h \setminus \{\mathbf{0}\}} \frac{a(\boldsymbol{u} - \boldsymbol{u}_h, \boldsymbol{v}_h) + b(\boldsymbol{v}_h, p - q_h)}{\|\nabla \boldsymbol{v}_h\|_{L^2(\Omega)}} \\
&\leqslant \frac{1}{\beta_h} \sup_{\boldsymbol{v}_h \in V_h \setminus \{\mathbf{0}\}} \frac{\nu \|\nabla(\boldsymbol{u} - \boldsymbol{u}_h)\|_{L^2(\Omega)} \|\nabla \boldsymbol{v}_h\|_{L^2(\Omega)} + \|\nabla \boldsymbol{v}_h\|_{L^2(\Omega)} \|p - q_h\|_{L^2(\Omega)}}{\|\nabla \boldsymbol{v}_h\|_{L^2(\Omega)}} \\
&\leqslant \frac{1}{\beta_h} \left(\nu \|\nabla(\boldsymbol{u} - \boldsymbol{u}_h)\|_{L^2(\Omega)} + \|p - q_h\|_{L^2(\Omega)} \right).
\end{aligned}$$

Inserting the error estimate (2.2.34) and plugging it into (2.2.42), we obtain the resulting error estimate for the L_2 norm of the pressure (2.2.41). ■

Theorem 2.2.6 (Error Estimate for the Velocity in $L^2(\Omega)$) To obtain the optimal error estimate for velocity in $L^2(\Omega)$, we introduce the dual Stokes equations. For given $\boldsymbol{f} \in \hat{L}^2(\Omega)$, find $(\boldsymbol{\phi}_{\hat{\boldsymbol{f}}}, \xi_{\hat{\boldsymbol{f}}}) \in V \times Q$ such that

$$-\nu \triangle \boldsymbol{\phi}_{\hat{\boldsymbol{f}}} - \nabla \xi_{\hat{\boldsymbol{f}}} = \hat{\boldsymbol{f}} \quad \text{in } \Omega, \tag{2.2.44}$$

$$\nabla \cdot \boldsymbol{\phi}_{\hat{\boldsymbol{f}}} = 0 \quad \text{in } \Omega. \tag{2.2.45}$$

Then the following error estimate for the velocity holds

$$\begin{aligned}
\|\boldsymbol{u} - \boldsymbol{u}_h\|_{L^2(\Omega)} &\leqslant \left(\|\nabla(\boldsymbol{u} - \boldsymbol{u}_h)\|_{L^2(\Omega)} + \nu^{-1} \inf_{q_h \in Q_h} \|p - q_h\|_{L^2(\Omega)} \right) \\
\times \sup_{\hat{\boldsymbol{f}} \in L^2(\Omega) \setminus \mathbf{0}} \frac{1}{\|\hat{\boldsymbol{f}}\|_{L^2(\Omega)}} &\left[\inf_{\boldsymbol{\phi}_h \in V_h^{div}} \|\nabla(\boldsymbol{\phi}_{\hat{\boldsymbol{f}}} - \boldsymbol{\phi}_h)\|_{L^2(\Omega)} + \inf_{r_h \in Q_h} \|\xi_{\hat{\boldsymbol{f}}} - r_h\|_{L^2(\Omega)} \right].
\end{aligned}$$

Proof: See [5], Theorem 4.28. ■

2.2.4 The Inf-Sup Stable Pairs of the Finite Element Spaces

The Taylor-Hood pairs which have been introduced firstly in [6] are a popular choice for solving incompressible fluid problems, as they have been proven to satisfy the discrete inf-sup condition (2.2.27) in two and three dimensions, see Theorems 8.1 and 8.2 of [7].

Definition 2.2.9 (The Family of Taylor–Hood Finite Element Spaces) Given a triangulation $\mathcal{T}_h$ of the domain $\Omega \in \mathbb{R}^d, d = 2, 3$. The family of Taylor–Hood finite element spaces on triangular grids is given by P_k/P_{k-1}, the k-th piecewise continuous polynomial spaces for the velocity space, and the $(k-1)$-th continuous piecewise polynomial spaces for the pressure space, which consist of

$$P_k(\mathcal{T}_h) = \left\{v_h \in C(\bar{\Omega}) : v_h \mid_K \in P_k, \forall K \in \mathcal{T}_h\right\}, \tag{2.2.46}$$

$$P_{k-1}(\mathcal{T}_h) = \left\{q_h \in C(\bar{\Omega}) : q_h \mid_K \in P_{k-1}, \forall K \in \mathcal{T}_h\right\}, \tag{2.2.47}$$

where $k \geqslant 2$. ▫

Remark 2.2.15 (Error Estimates for Taylor-Hood Pairs of Finite Element Spaces) Consider the discrete Stokes equation (2.2.26) with Taylor-Hood pairs of Finite Element Spaces, assume the unique solution $(\boldsymbol{u}, p)$ of (2.2.5) lies in $H^m(\Omega) \times H^{m-1}(\Omega)$, then the following errors hold

$$\|\nabla(\boldsymbol{u} - \boldsymbol{u}_h)\|_{L^2(\Omega)} \leqslant Ch^k \left(\|\boldsymbol{u}\|_{H^{k+1}(\Omega)} + \nu^{-1}\|p\|_{H^k(\Omega)}\right), \tag{2.2.48}$$

$$\|\nabla \cdot \boldsymbol{u}_h\|_{L^2(\Omega)} \leqslant Ch^k \left(\|\boldsymbol{u}\|_{H^{k+1}(\Omega)} + \nu^{-1}\|p\|_{H^k(\Omega)}\right), \tag{2.2.49}$$

$$\|\boldsymbol{u} - \boldsymbol{u}_h\|_{L^2(\Omega)} \leqslant Ch^{k+1} \left(\|\boldsymbol{u}\|_{H^{k+1}(\Omega)} + \nu^{-1}\|p\|_{H^k(\Omega)}\right), \tag{2.2.50}$$

$$\|p - p_h\|_{L^2(\Omega)} \leqslant Ch^k \left(\nu\|\boldsymbol{u}\|_{H^{k+1}(\Omega)} + \|p\|_{H^k(\Omega)}\right), \tag{2.2.51}$$

with a constant C depends on the inverse of constant β_h in the discrete inf-sup condition (2.2.27).

Remark 2.2.16 The error estimates (2.2.48), (2.2.49), and (2.2.50) reveal that when the viscosity is small, the error estimate for velocity will become large, while the error estimate for pressure will be small, as shown in (2.2.51). The pressure terms in the velocity error estimates arise due to the fact that the discrete finite element space is not weakly divergence-free, i.e., $V_h^{div} \not\subset V^{div}$, which means that the conservation of mass cannot be guaranteed. This leads to a pressure-dependent consistency error that affects the computed velocity and is known as the lack of pressure-robustness, as discussed in [8]. To address this issue, we introduce the grad-div stabilization method, which is applied to the Taylor-Hood finite element method. In the next chapter, we will present a discretization that improves the mass conservation property. ▫

Chapter 3

Grad-Div Stabilizations for the Stokes Problem

3.1 Standard Grad-Div Stabilization

In fluid mechanics, the mass conservation is a fundamental law. A numerical algorithm used to solve fluid problems should satisfy this property in order to obtain physically accurate results. Therefore, in this chapter, we investigate the use of the grad-div stabilization method which is known to improve the mass conservation property of the numerical solution.
In recent decades, the grad-div stabilization method has been extensively researched in theoretical and computational aspects, see [9], [10] and [11]. This simple and practical technique was first proposed for the incompressible flow in [12], and it adds a stabilization term $\gamma\nabla\nabla\cdot\boldsymbol{u}$ to the momentum equation, which does not affect the solution of the continuum problem since the stabilization term is zero. Utilizing the Galerkin finite element method mentioned in the last chapter, the term $\gamma(\nabla\cdot\boldsymbol{u}_h, \nabla\cdot\boldsymbol{u}_h)$ is obtained by replacing the infinite-dimensional space with the finite-dimensional space through integration by parts in the weak formulation. For most of the common choices of finite element pairs like Taylor-Hood, $\nabla\cdot\boldsymbol{u}_h \neq 0$, thus the grad-div stabilization term is not zero in the finite element discretization. It can influence the discrete solution, which in turn improves the mass conservation in the finite element method, and also further increases the accuracy of the approximate solution of the Stokes equations by reducing the effect of pressure on the velocity error, see [10] and [13].

Definition 3.1.1 (The Grad-Div Stabilization) The weak formulation of the Stokes equations (2.2.2) is extended with the grad-div stabilization term. Then, the stabilized finite element discretization is represented as follows: for fixed $\gamma > 0$, find the solution $(\boldsymbol{u}_h, p_h) \in V_h \times Q_h$, for all $(\boldsymbol{v}_h, q_h) \in V_h \times Q_h$ such that

$$\begin{aligned} \nu(\nabla \boldsymbol{u}_h, \nabla \boldsymbol{v}_h) + \gamma(\nabla \cdot \boldsymbol{u}_h, \nabla \cdot \boldsymbol{v}_h) - (\nabla \cdot \boldsymbol{v}_h, p_h) &= (\boldsymbol{f}, \boldsymbol{v}_h), \\ (\nabla \cdot \boldsymbol{u}_h, q_h) &= 0. \end{aligned} \tag{3.1.1}$$

Here, γ is the stabilization parameter. □

Remark 3.1.1 Let

$$\tilde{a}_h(\boldsymbol{u}_h, \boldsymbol{v}_h) = \nu(\nabla \boldsymbol{u}_h, \nabla \boldsymbol{v}_h) + \gamma(\nabla \cdot \boldsymbol{u}_h, \nabla \cdot \boldsymbol{v}_h), \tag{3.1.2}$$

on the left-hand side of the (3.1.1), the first term is positive definite, and the second term is semi-positive definite. Thus, the bilinear form $\tilde{a}_h(\cdot, \cdot)$ is coercive. The existence and uniqueness of the solution of (3.1.1) could be proved in a similar way as Corollary 2.2.1. □

Remark 3.1.2 (The linear system of the Stokes Problem) Assembling the discretized equations

$$\begin{aligned} \tilde{a}_h(\boldsymbol{u}_h, \boldsymbol{v}_h) + b_h(p_h, \boldsymbol{v}_h) &= F(\boldsymbol{v}_h), \\ b_h(\boldsymbol{u}_h, q_h) &= 0, \end{aligned} \tag{3.1.3}$$

which results in a linear system of the form like (2.2.30),

$$\begin{pmatrix} \tilde{A}_h & B_h^T \\ B_h & 0 \end{pmatrix} \begin{pmatrix} \underline{u} \\ \underline{p} \end{pmatrix} = \begin{pmatrix} \underline{f} \\ 0 \end{pmatrix}, \tag{3.1.4}$$

where

$$\begin{aligned} &\tilde{A}_h = (\tilde{a}_{ij})_{N \times N} \text{ with} \\ &(\tilde{a}_{ij}) := a(\boldsymbol{\phi}_j, \boldsymbol{\phi}_i) = \sum_{K \in \mathcal{T}_h} \nu(\nabla \boldsymbol{\phi}_j, \nabla \boldsymbol{\phi}_i)_K + \sum_{K \in \mathcal{T}_h} \gamma_K(\nabla \cdot \boldsymbol{\phi}_j, \nabla \cdot \boldsymbol{\phi}_i)_K, \end{aligned}$$

where $i, j = 1, .., 3N$, and the stabilization parameters are $\{\gamma_K\}$ with $\gamma_K > 0$. Applying the grad-div stabilization, the matrix $\tilde{A}_h$ has the following form

$$\tilde{A}_h = \begin{pmatrix} A_{11} & 0 & 0 \\ 0 & A_{11} & 0 \\ 0 & 0 & A_{11} \end{pmatrix} + \begin{pmatrix} \tilde{A}_{11} & \tilde{A}_{12} & \tilde{A}_{13} \\ \tilde{A}_{21} & \tilde{A}_{22} & \tilde{A}_{23} \\ \tilde{A}_{31} & \tilde{A}_{32} & \tilde{A}_{33} \end{pmatrix}, \tag{3.1.5}$$

where the matrix entries are

$$(\tilde{A}_{kl})_{ij} = \gamma(\partial_l \phi_j, \partial_k \phi_i), \ k, l = 1, \cdots, d, \ i, j = 1, \cdots, 3N.$$

The symmetry of the off-diagonal blocks of $\tilde{A}_h$ follows directly from the symmetry of the grad-div term. The grad-div term affects only the velocity-velocity coupling, and thus using this term will make A_h block-full. □

Lemma 3.1.1 (Stability of the Solution) The solution of the Stokes equation with the grad-div stabilization (3.1.1) exists uniquely and satisfies

$$\nu\|\nabla \boldsymbol{u}_h\|_{L^2(\Omega)}^2 + 2\gamma\|\nabla \cdot \boldsymbol{u}_h\|_{L^2(\Omega)}^2 \leqslant \nu^{-1}\|\boldsymbol{f}\|_{H^{-1}(\Omega)}^2. \tag{3.1.6}$$

Proof: Choosing the test function $\boldsymbol{v}_h = \boldsymbol{u}_h$ in (3.1.1) yields

$$\nu\|\nabla \boldsymbol{u}_h\|_{L^2(\Omega)}^2 + \gamma\|\nabla \cdot \boldsymbol{u}_h\|_{L^2(\Omega)}^2 = (\boldsymbol{f}, \boldsymbol{u}_h). \tag{3.1.7}$$

On the right-hand side of the equation, using Cauchy-Schwarz and Young's inequality, one obtains

$$\nu\|\nabla \boldsymbol{u}_h\|_{L^2(\Omega)}^2 + \gamma\|\nabla \cdot \boldsymbol{u}_h\|_{L^2(\Omega)}^2 \leqslant \frac{\nu^{-1}}{2}\|\boldsymbol{f}\|_{H^{-1}(\Omega)}^2 + \frac{\nu}{2}\|\nabla \boldsymbol{u}_h\|_{L^2(\Omega)}^2. \tag{3.1.8}$$

Eliminating the same term and multiplying both sides by 2, the final result is proved. ■

Remark 3.1.3 The Lemma 3.1.1 indicates that the grad-div stabilization with the parameter γ can effectively control the divergence error. □

Definition 3.1.2 (Optimal Approximation Property of a Sequence of Divergence-free Subspaces) Consider a sequence of triangulations $\{\mathcal{T}_h\}$ with characteristic mesh size h and the corresponding space $V_{h,0} := \{\boldsymbol{v}_h \in V_h, \nabla \cdot \boldsymbol{v}_h = 0\}$. If for all the solenoidal $\boldsymbol{v}_h \in V_h \cap H^{k+1}(\Omega)$,

$$\inf_{\boldsymbol{v}_h \in V_{h.0}} \|\nabla(\boldsymbol{v} - \boldsymbol{v}_h)\|_{L^2(\Omega)} \leqslant C_{div} \inf_{\boldsymbol{v}_h \in V_h} \|\nabla(\boldsymbol{v} - \boldsymbol{v}_h)\|_{H^{k+1}(\Omega)}, \tag{3.1.9}$$

where the constant C_{div} is independent of h, then the sequence of spaces $V_{h,0}$ is said to possess optimal approximation properties.

Remark 3.1.4 Whether the sequence possesses the optimal approximation property influenced by the pair of inf-sup stable finite element spaces and the triangulation of the domain, which is not expected to exist in the general case. However, there are special cases such as Taylor–Hood pair of spaces P_k/P_{k-1} with $k \geqslant d$ on barycentric-refined simplicial grids in [14].

□

Theorem 3.1.1 (Error Estimate for the Velocity in Standard Grad-Div Stabilization) Let $(\boldsymbol{u}_h, p_h) \in V_h \times Q_h$ be the discrete approximation solution to the Stokes equation (2.2.1) with grad-div stabilization. The finite element error in the L^2 norm of the velocity gradient and the divergence is

$$\|\nabla(\boldsymbol{u} - \boldsymbol{u}_h)\|_{L^2(\Omega)}^2 + \frac{\gamma}{2\nu}\|\nabla \cdot (\boldsymbol{u} - \boldsymbol{u}_h)\|_{L^2(\Omega)}^2 \leqslant$$

$$\inf_{\boldsymbol{v}_h \in V_h^{div}} \left(4\|\nabla(\boldsymbol{u} - \boldsymbol{v}_h)\|_{L^2(\Omega)}^2 + \frac{3\gamma}{\nu}\|\nabla \cdot (\boldsymbol{u} - \boldsymbol{v}_h)\|_{L^2(\Omega)}^2\right) + \frac{4}{\nu\gamma} \inf_{q_h \in Q_h} \|p - q_h\|_{L^2(\Omega)}^2. \tag{3.1.10}$$

Proof: Consider $\boldsymbol{u} - \boldsymbol{u}_h = (\boldsymbol{u} - \boldsymbol{v}_h) + (\boldsymbol{v}_h - \boldsymbol{u}_h) =: \boldsymbol{\eta} + \boldsymbol{\phi}_h$, for all $\boldsymbol{v}_h \in V_h^{div}$, one obtains the following equation by subtracting discrete equations (3.1.1) from the original (2.2.5),

$$\begin{aligned}\nu(\nabla\boldsymbol{\phi}_h, \nabla\boldsymbol{v}_h) + \gamma(\nabla\cdot\boldsymbol{\phi}_h, \nabla\cdot\boldsymbol{v}_h) = &-\nu(\nabla\boldsymbol{\eta}, \nabla\boldsymbol{v}_h) - \gamma(\nabla\cdot\boldsymbol{\eta}, \nabla\cdot\boldsymbol{v}_h)\\ &+ (\nabla\cdot\boldsymbol{v}_h, p).\end{aligned} \tag{3.1.11}$$

Since $(\nabla\cdot\boldsymbol{v}_h, q_h) = 0, \forall q_h \in Q_h$, this term can be added in the right-hand side of the equation (3.1.11). Choosing $\boldsymbol{v}_h = \boldsymbol{\phi}_h$, then (3.1.11) becomes

$$\begin{aligned}\nu\|\nabla\boldsymbol{\phi}_h\|^2_{L^2(\Omega)} + \gamma\|\nabla\cdot\boldsymbol{\phi}_h\|^2_{L^2(\Omega)} = &-\nu(\nabla\boldsymbol{\eta}, \nabla\boldsymbol{\phi}_h) - \gamma(\nabla\cdot\boldsymbol{\eta}, \nabla\cdot\boldsymbol{\phi}_h)\\ &+ (\nabla\cdot\boldsymbol{\phi}_h, p - q_h).\end{aligned} \tag{3.1.12}$$

Applying the Cauchy-Schwarz and Young's inequality ($p = q = \frac{1}{2}$), one obtains

$$\begin{aligned}\nu\|\nabla\boldsymbol{\phi}_h\|^2_{L^2(\Omega)} + \gamma\|\nabla\cdot\boldsymbol{\phi}_h\|^2_{L^2(\Omega)} \leqslant &\nu\|\nabla\boldsymbol{\eta}\|^2_{L^2(\Omega)} + \gamma\|\nabla\cdot\boldsymbol{\eta}\|^2_{L^2(\Omega)}\\ &+ 2\|p - q_h\|_{L^2(\Omega)}\|\nabla\cdot\boldsymbol{\phi}_h\|_{L^2(\Omega)}.\end{aligned} \tag{3.1.13}$$

The right-hand side of the equation can be estimated by the Peter-Paul inequality, then

$$2\|p - q_h\|_{L^2(\Omega)}\|\nabla\cdot\boldsymbol{\phi}_h\|_{L^2(\Omega)} \leqslant 2\gamma^{-1}\|p - q_h\|^2_{L^2(\Omega)} + \frac{\gamma}{2}\|\nabla\cdot\boldsymbol{\phi}_h\|^2_{L^2(\Omega)}. \tag{3.1.14}$$

which results

$$\begin{aligned}\|\nabla\boldsymbol{\phi}_h\|^2_{L^2(\Omega)} + \frac{\gamma}{2\nu}\|\nabla\cdot\boldsymbol{\phi}_h\|^2_{L^2(\Omega)} \leqslant &\|\nabla\boldsymbol{\eta}\|^2_{L^2(\Omega)} + \frac{\gamma}{\nu}\|\nabla\cdot\boldsymbol{\eta}\|^2_{L^2(\Omega)}\\ &+ \frac{2}{\gamma\nu}\inf_{q_h\in Q_h}\|p - q_h\|^2_{L^2(\Omega)}.\end{aligned} \tag{3.1.15}$$

By the triangle inequality and Young's inequality ($p = q = \frac{1}{2}$), one gets

$$\begin{aligned}&\|\nabla(\boldsymbol{u} - \boldsymbol{u}_h)\|^2_{L^2(\Omega)} + \frac{\gamma}{2\nu}\|\nabla\cdot(\boldsymbol{u} - \boldsymbol{u}_h)\|^2_{L^2(\Omega)} \leqslant\\ &\inf_{\boldsymbol{v}_h\in V_h^{div}}\left(4\|\nabla\boldsymbol{\eta}\|^2_{L^2(\Omega)} + \frac{3\gamma}{\nu}\|\nabla\cdot\boldsymbol{\eta}\|^2_{L^2(\Omega)}\right) + \frac{4}{\nu\gamma}\inf_{q_h\in Q_h}\|p - q_h\|^2_{L^2(\Omega)}.\end{aligned} \tag{3.1.16}$$

which gives the final error estimate, for all $\boldsymbol{v}_h \in V_h^{div}$. ∎

Remark 3.1.5 If the grad-div stabilization finite element method with the Taylor-Hood pairs possesses the optimal approximation property. By standard approximation theory in [15], we have that

$$\|\nabla(\boldsymbol{u}-\boldsymbol{u}_h)\|^2_{L^2(\Omega)} + \frac{\gamma}{2\nu}\|\nabla\cdot(\boldsymbol{u}-\boldsymbol{u}_h)\|^2_{L^2(\Omega)} \leqslant Ch^{2k}\left(|\boldsymbol{u}|^2_{k+1} + \frac{1}{\nu\gamma}|p|^2_k\right). \tag{3.1.17}$$

The error estimate (3.1.17) suggests that the choice of the parameter γ can influence the error bound. A larger value of γ can be chosen without increasing the error bound. Moreover, as the value of γ increases, the impact of the pressure term on the error can be reduced to some extent. □

Theorem 3.1.2 (Error Estimate for the Pressure) Let $(\boldsymbol{u}_h, p) \in V_h \times Q_h$ be the discrete approximation solution of the Stokes equation (2.2.1) with grad-div stabilization and assume the inf-sup constant $0 < \beta \leqslant \mathcal{O}(1)$. For $\boldsymbol{v}_h$ in the discretely divergence-free space $V_{0,h}$, the pressure error is bounded by

$$\begin{aligned}\|p-p_h\|^2_{L^2(\Omega)} \leqslant C(\beta^{-1})\Bigg\{&\left(1+\left(\frac{\nu}{\gamma}\right)^{1/2}\right)\inf_{q_h\in Q_h}\|p-q_h\|_{L^2(\Omega)}\\ &+\inf_{\boldsymbol{v}_h\in V_{0,h}}\left(\nu+(\nu\gamma)^{1/2}\right)\|\nabla(\boldsymbol{u}-\boldsymbol{v}_h)\|_{L^2(\Omega)}\\ &+\left((\nu\gamma)^{1/2}+\gamma\right)\|\nabla\cdot\boldsymbol{v}_h)\|_{L^2(\Omega)}\Bigg\}.\end{aligned} \tag{3.1.18}$$

Proof: See [11]. ■

Remark 3.1.6 The paper [11] analyzes the optimal choices of the grad-div stabilization parameters based on (3.1.11) and (3.1.18). By possessing optimal properties, one can see to what extent the violation of the conservation of mass is reduced using the grad-div stabilization method.
Overall, the grad-div stabilization method reduces the impact of the inverse of the viscosity and pressure on the error bound compared to Galerkin discrete methods. However, it does not entirely eliminate this effect. Too large values of the stabilization parameter can lead to over-stabilizing the problem, resulting in increased computational time in solving the corresponding linear algebraic system. □

3.2 Sparse Grad-Div Stabilization

Although the standard grad-div stabilization is considered effective in improving the mass conservation of the finite element method, the fully coupled block matrices (i.e., block-full) produced by it increase the coupling in the linear system. And the matrix arising from the stabilization terms is singular, which leads to a linear algebraic system that is more difficult to solve in [16]. In order to increase the sparsity of the matrix and reduce the coupling of the velocity coefficient matrix generated by the stabilization terms, a sparse grad-div stabilization method is proposed, see [17] and [18]. This new divergence operator, which has a similar positive effect on the error as standard grad-div stabilization, penalizing the lack of mass conservation, reduces the effect of the pressure error on the velocity error. It can improve the efficiency of the solution compared to the standard grad-div operator since the matrix is sparse.

Definition 3.2.1 Let $\Omega \in \mathbb{R}^d$, $d = 2$ or 3 be a bounded domain, and $\boldsymbol{u}, \boldsymbol{v} \in H^1(\Omega)$. The sparse grad-div stabilization (i.e., divergence penalization) operator g is defined by

$$g_{2d}(\boldsymbol{u}, \boldsymbol{v}) = \int_\Omega (u_{1_x} v_{1_x} + u_{2_y} v_{2_y} + 2u_{2_y} v_{1_x}), \tag{3.2.1}$$

$$\begin{aligned} g_{3d}(\boldsymbol{u}, \boldsymbol{v}) = &\int_\Omega (u_{1_x} v_{1_x} + u_{2_y} v_{2_y} + u_{3_z} v_{3_z} \\ &+ 2u_{2_y} v_{1_x} + 2u_{3_z} v_{1_x} + u_{3_z} v_{2_y} + u_{2_y} v_{3_z}). \end{aligned} \tag{3.2.2}$$

There is no interaction between the u_1 and v_2 functions in (3.2.1), which means the resulting matrix is upper triangular. In (3.2.2), the u_1 function has no interaction with v_2 or v_3, which reveals the 2,1 and 3,1 blocks are empty of the formed 3×3 block matrix. This is different from the standard grad-div operator

$$\text{grad-div}(\boldsymbol{u}, \boldsymbol{v}) = \int_\Omega (u_{1_x} + u_{2_y} + u_{3_z})(v_{1_x} + v_{2_y} + v_{3_z}), \tag{3.2.3}$$

which gives the full block matrix. □

Lemma 3.2.1 Define the $L^2(\Omega)$ inner product $(\boldsymbol{u}, \boldsymbol{v}) := \int_\Omega \boldsymbol{u}\boldsymbol{v} dx$. The operator g has the following properties which imply the positive impact it has on the incompressible flow simulation:

1. The operator g can be written as

$$g_{2d}(\boldsymbol{u},\boldsymbol{v}) = (\nabla\cdot\boldsymbol{u},\nabla\cdot\boldsymbol{v}) - (u_{1_x}, v_{2_y}) + (u_{2_y}, v_{1_x}), \tag{3.2.4}$$

$$\begin{aligned} g_{3d}(\boldsymbol{u},\boldsymbol{v}) = (\nabla\cdot\boldsymbol{u},\nabla\cdot\boldsymbol{v}) - (u_{1_x}, v_{2_y}) + (u_{2_y}, v_{1_x}) \\ - (u_{1_x}, v_{3_z}) + (u_{3_z}, v_{1_x}). \end{aligned} \tag{3.2.5}$$

2. The operator g satisfied

$$g(\boldsymbol{u},\boldsymbol{u}) = \|\nabla\cdot\boldsymbol{u}\|^2, \tag{3.2.6}$$

   in 2d and 3d.

3. If $\nabla\cdot\boldsymbol{u}=0$, then in 2d or 3d

$$g(\boldsymbol{u},\boldsymbol{v}) = -(u_{1_x},\nabla\cdot\boldsymbol{v}). \tag{3.2.7}$$

Proof: Using the definition (3.2.1) of sparse grad-div stabilization, combing the $L^2(\Omega)$ inner product, one can easily get the (3.2.4) and (3.2.5). For (3.2.6), let $\boldsymbol{u}=\boldsymbol{v}$, the result is trivially obtained.
For (3.2.7) in 2d form, since $\nabla\cdot\boldsymbol{u}=0$, let $u_{1_x}=-u_{2_y}$, we have

$$\begin{aligned} g_{2d}(\boldsymbol{u},\boldsymbol{v}) &= (\nabla\cdot\boldsymbol{u},\nabla\cdot\boldsymbol{v}) - (u_{1_x}, v_{2_y}) + (u_{2_y}, v_{1_x}) \\ &= -(u_{1_x}, v_{2_y}) + (u_{2_y}, v_{1_x}) \\ &= -(u_{1_x}, v_{2_y}) + (-u_{1_x}, v_{1_x}) \\ &= -(u_{1_x},\nabla\cdot\boldsymbol{v}). \end{aligned}$$

To prove (3.2.7) in 3d form, we use a similar way as in the 2d form. Let $u_{1_x}=-u_{2_y}-u_{3_z}$, we get

$$\begin{aligned} g_{3d}(\boldsymbol{u},\boldsymbol{v}) &= (\nabla\cdot\boldsymbol{u},\nabla\cdot\boldsymbol{v}) - (u_{1_x}, v_{2_y}) + (u_{2_y}, v_{1_x}) - (u_{1_x}, v_{3_z}) + (u_{3_z}, v_{1_x}) \\ &= -(u_{1_x}, v_{2_y}) + (u_{2_y}, v_{1_x}) - (u_{1_x}, v_{3_z}) + (u_{3_z}, v_{1_x}) \\ &= (u_{2_y}+u_{3_z}, v_{1_x}) - (u_{1_x}, v_{2_y}) - (u_{1_x}, v_{3_z}) \\ &= (-u_{1_x}, v_{1_x}) - (u_{1_x}, v_{2_y}) - (u_{1_x}, v_{3_z}) \\ &= -(u_{1_x},\nabla\cdot\boldsymbol{v}) \end{aligned}$$

Thus, Lemma 3.2.1 is now completely proved. ■

Remark 3.2.1 From Lemma 3.2.1, the results suggest that the sum of grad-div stabilization and the gradient of u_{1_x} in the weak formulation interprets the operator g in another way. For divergence-free $\boldsymbol{u}$ and $\boldsymbol{v} \in H_0^1(\Omega)$, it holds that

$$-\nabla(\nabla \cdot \boldsymbol{u}), \boldsymbol{v}) + (\nabla u_{1_x}, \boldsymbol{v}) = (\nabla \cdot \boldsymbol{u}, \nabla \cdot \boldsymbol{v}) - (u_{1_x}, \nabla \cdot \boldsymbol{v}) = g(\boldsymbol{u}, \boldsymbol{v}). \quad (3.2.8)$$

In this case, the gradient terms can be added to the true pressure to create a modified pressure $P = p + \gamma u_{1_x}$ that has no impact on the velocity solution. The most common use is the Bernoulli pressure $P_{Bernoulli} = p + |u|^2/2$ when computing with rotation form of the Navier-Stokes equations, see [19]. □

Remark 3.2.2 By analysing (3.2.8), the gradient term of u_{1_x} could be replace by the u_{2_y} in 2d, u_{2_y} or u_{3_z} in 3d as follows by defining

$$g_{2d}(\boldsymbol{u}, \boldsymbol{v}) = \int_\Omega (u_{1_x} v_{1_x} + u_{2_y} v_{2_y} + 2u_{1_x} v_{2_y}), \quad (3.2.9)$$

$$\begin{aligned} g_{3d}(\boldsymbol{u}, \boldsymbol{v}) = &\int_\Omega (u_{1_x} v_{1_x} + u_{2_y} v_{2_y} + u_{3_z} v_{3_z} \\ &+ 2u_{1_x} v_{2_y} + 2u_{3_z} v_{2_y} + u_{3_z} v_{1_x} + u_{1_x} v_{3_z}), \end{aligned} \quad (3.2.10)$$

or

$$\begin{aligned} g_{3d}(\boldsymbol{u}, \boldsymbol{v}) = &\int_\Omega (u_{1_x} v_{1_x} + u_{2_y} v_{2_y} + u_{3_z} v_{3_z} \\ &+ 2u_{1_x} v_{3_z} + 2u_{2_y} v_{3_z} + u_{2_y} v_{1_x} + u_{1_x} v_{2_y}) \end{aligned} \quad (3.2.11)$$

The (3.2.9), (3.2.10) and (3.2.11) also have the same properties in Lemma 3.2.1:

1. The operator can be written as

$$g_{2d}(\boldsymbol{u}, \boldsymbol{v}) = (\nabla \cdot \boldsymbol{u}, \nabla \cdot \boldsymbol{v}) - (u_{2_y}, v_{1_x}) + (u_{1_x}, v_{2_y}),$$

$$\begin{aligned} g_{3d}(\boldsymbol{u}, \boldsymbol{v}) = (\nabla \cdot \boldsymbol{u}, \nabla \cdot \boldsymbol{v}) &- (u_{2_y}, v_{1_x}) - (u_{2_y}, v_{3_z}) \\ &+ (u_{1_x}, v_{2_y}) + (u_{3_z}, v_{2_y}), \end{aligned}$$

or

$$\begin{aligned} g_{3d}(\boldsymbol{u}, \boldsymbol{v}) = (\nabla \cdot \boldsymbol{u}, \nabla \cdot \boldsymbol{v}) &- (u_{3_z}, v_{1_x}) - (u_{3_z}, v_{2_y}) \\ &+ (u_{1_x}, v_{3_z}) + (u_{2_y}, v_{3_z}). \end{aligned}$$

2. The operator g satisfied

$$g(\boldsymbol{u}, \boldsymbol{u}) = \|\nabla \cdot \boldsymbol{u}\|^2, \tag{3.2.12}$$

in 2d and 3d.

3. If $\nabla \cdot \boldsymbol{u} = 0$, then in 2d or 3d

$$g(\boldsymbol{u}, \boldsymbol{v}) = -(u_{2_y}, \nabla \cdot \boldsymbol{v}), \tag{3.2.13}$$

or

$$g(\boldsymbol{u}, \boldsymbol{v}) = -(u_{3_z}, \nabla \cdot \boldsymbol{v}) \tag{3.2.14}$$

in 3d.

The proof is similar to that of Lemma 3.2.1. The empty blocks will also appear in the velocity matrix but in different locations. In the solution of practical problems, it is expected to get a better-modified pressure by adding the smallest term of u_{1_x}, u_{2_y}, and u_{3_z} in [20]. □

Remark 3.2.3 As the matrix in (3.1.5), in order to represent the sparse grad-div matrix $\bar{A}_h$, we write the discrete divergence operator in its three components $X^T = (X_1^T, X_2^T, X_3^T) \in \mathbb{R}^{N \times 3N}$ corresponding to the derivatives in the three spatial directions. For a given non-singular matrix $M \in \mathbb{R}^{N \times N}$, the matrix $\bar{A}_h$ has the following form:

$$\bar{A}_h = \begin{pmatrix} A_{11} & 0 & 0 \\ 0 & A_{11} & 0 \\ 0 & 0 & A_{11} \end{pmatrix} + \gamma \begin{pmatrix} X_1 M^{-1} X_1^T & 2X_1 M^{-1} X_2^T & 2X_1 M^{-1} X_3^T \\ 0 & X_2 M^{-1} X_2^T & X_2 M^{-1} X_3^T \\ 0 & X_3 M^{-1} X_2^T & X_3 M^{-1} X_3^T \end{pmatrix}.$$

In this way, the standard grad-div matrix $\tilde{A}_h$ can be written as

$$\tilde{A}_h = \begin{pmatrix} A_{11} & 0 & 0 \\ 0 & A_{11} & 0 \\ 0 & 0 & A_{11} \end{pmatrix} + \gamma X M^{-1} X^T.$$

□

Definition 3.2.2 (The Stokes Equation with Sparse Grad-Div Operator g) For the fixed stabilization parameter $\gamma > 0$, the weak formulation of the Stokes equations (2.2.2) with the sparse grad-div operator is given by: find the solution $(\boldsymbol{u}_h, p_h) \in V_h \times Q_h$, for all $(\boldsymbol{v}_h, q_h) \in V_h \times Q_h$ such that

$$\nu(\nabla \boldsymbol{u}_h, \nabla \boldsymbol{v}_h) + \gamma g(\boldsymbol{u}_h, \boldsymbol{v}_h) - (\nabla \cdot \boldsymbol{v}_h, p_h) = (\boldsymbol{f}, \boldsymbol{v}_h), \tag{3.2.15}$$

$$(\nabla \cdot \boldsymbol{u}_h, q_h) = 0. \tag{3.2.16}$$

It needs to be noted that the pressure p_h in (3.2.15) is not the approximation to the Stokes equation, since a modified pressure $p + \gamma u_{1_x}$ is created, and this modified pressure converges optimally to the true Stokes pressure.

Theorem 3.2.1 (Error Estimate for the Velocity in Sparse Grad-Div Stabilization) Let $(\boldsymbol{u}_h, p_h) \in V_h \times Q_h$ be the discrete approximation solution of the Stokes equation (2.2.1) with sparse grad-div stabilization, the L^2 norm of the velocity gradient and the divergence is bounded by

$$\begin{aligned} \|\nabla(\boldsymbol{u}-\boldsymbol{u}_h)\|^2_{L^2(\Omega)} + \frac{\gamma}{\nu}\|\nabla\cdot(\boldsymbol{u}-\boldsymbol{u}_h)\|^2_{L^2(\Omega)} \leqslant \frac{2}{\gamma\nu}\inf_{q_h\in Q_h}\|p-\gamma u_{1_x}-q_h\|^2_{L^2(\Omega)} \\ + \inf_{\boldsymbol{v}_h\in V_h^{div}}\left\{\frac{2\gamma}{\nu}\|\nabla\cdot\boldsymbol{v}_h\|^2_{L^2(\Omega)} + \left(6+\frac{4\gamma^2}{\nu^2}\right)\|\nabla(\boldsymbol{u}-\boldsymbol{v}_h)\|^2_{L^2(\Omega)}\right\}. \end{aligned} \tag{3.2.17}$$

□

Proof: The proof is similar to Theorem 3.1.1, let $\boldsymbol{u}-\boldsymbol{u}_h = (\boldsymbol{u}-\boldsymbol{v}_h) + (\boldsymbol{v}_h - \boldsymbol{u}_h) =: \boldsymbol{\eta} + \boldsymbol{\phi}_h$, where $\boldsymbol{v}_h \in V_h^{div}$.
Add the sparse operator $\gamma g(\boldsymbol{u}, \boldsymbol{v}_h)$ to both sides of the variational form of the Stokes equations (2.2.2). Since $\nabla\cdot\boldsymbol{u} = 0$, using the property (3.2.7) from Lemma 3.2.1, one gets

$$\begin{aligned} \nu(\nabla\boldsymbol{u}, \nabla\boldsymbol{v}_h) + \gamma g(\boldsymbol{u}, \boldsymbol{v}_h) - (\nabla\cdot\boldsymbol{v}_h, p) \\ = (\boldsymbol{f}, \boldsymbol{v}_h) - \gamma(u_{1_x}, \nabla\cdot\boldsymbol{v}_h). \end{aligned} \tag{3.2.18}$$

By subtracting (3.2.15) from (3.2.18), one obtains

$$\nu(\nabla(\boldsymbol{u}-\boldsymbol{u}_h), \nabla\boldsymbol{v}_h) + \gamma g((\boldsymbol{u}-\boldsymbol{u}_h), \boldsymbol{v}_h) = (\nabla\cdot\boldsymbol{v}_h, p - \gamma u_{1_x}). \tag{3.2.19}$$

Using the decomposition of $\boldsymbol{u}-\boldsymbol{u}_h$, and choosing $\boldsymbol{v}_h = \boldsymbol{\phi}_h$, So we modify our error equation as

$$\begin{aligned} \nu\|\nabla\boldsymbol{\phi}_h\|^2_{L^2(\Omega)} + \gamma\|\nabla\cdot\boldsymbol{\phi}_h\|^2_{L^2(\Omega)} = -\nu(\nabla\boldsymbol{\eta}, \nabla\boldsymbol{\phi}_h) \\ - \gamma g(\boldsymbol{\eta}, \boldsymbol{\phi}_h) + (\nabla\cdot\boldsymbol{\phi}_h, p - \gamma u_{1_x} - q_h), \ \forall q_h \in Q_h. \end{aligned} \tag{3.2.20}$$

We will take the absolute value of the right-hand side of (3.2.20) and treat each term separately.
Then, for the first and third terms on the right-hand side of the equation (3.2.20), using Cauchy-Schwarz inequality and Young's inequality, the estimates are obtained as follows

$$\begin{aligned} |\nu(\nabla\boldsymbol{\eta}, \nabla\boldsymbol{\phi}_h)| &\leqslant \nu\|\nabla\boldsymbol{\eta}\|_{L^2(\Omega)}\|\nabla\boldsymbol{\phi}_h\|_{L^2(\Omega)} \\ &\leqslant \nu\|\nabla\boldsymbol{\eta}\|^2_{L^2(\Omega)} + \frac{\nu}{4}\|\nabla\boldsymbol{\phi}_h\|^2_{L^2(\Omega)}, \end{aligned} \tag{3.2.21}$$

$$
\begin{aligned}
|(\nabla \cdot \boldsymbol{\phi}_h, p - \gamma u_{1_x} - q_h)| &\leqslant \|\nabla \cdot \boldsymbol{\phi}_h\|_{L^2(\Omega)} \|p - \gamma u_{1_x} - q_h\|_{L^2(\Omega)} \\
&\leqslant \frac{\gamma}{2} \|\nabla \cdot \boldsymbol{\phi}_h\|^2_{L^2(\Omega)} + \frac{1}{2\gamma} \|p - \gamma u_{1_x} - q_h\|^2_{L^2(\Omega)}.
\end{aligned}
\tag{3.2.22}
$$

To bound the g function on the right-hand side of (3.2.20), we also use the properties of the g operator from Lemma 3.2.1, to get

$$
\begin{aligned}
|\gamma g(\boldsymbol{\eta}, \boldsymbol{\phi_h})| \leqslant \gamma \|\nabla \boldsymbol{\eta}\|_{L^2(\Omega)} \|\nabla \boldsymbol{\phi}_h\|_{L^2(\Omega)} &\leqslant \frac{\nu}{4} \|\nabla \boldsymbol{\phi}_h\|^2_{L^2(\Omega)} \\
&+ \frac{\gamma^2}{\nu} \|\nabla \boldsymbol{\eta}\|^2_{L^2(\Omega)},
\end{aligned}
\tag{3.2.23}
$$

and combining this estimate with (3.2.21) and (3.2.22), then it gives

$$
\begin{aligned}
\|\nabla \boldsymbol{\phi}_h\|^2_{L^2(\Omega)} + \frac{\gamma}{\nu} \|\nabla \cdot \boldsymbol{\phi}_h\|^2_{L^2(\Omega)} &\leqslant \left(2 + \frac{2\gamma^2}{\nu^2}\right) \|\nabla \boldsymbol{\eta}\|^2_{L^2(\Omega)} \\
&+ \frac{1}{\gamma \nu} \inf_{q_h \in Q_h} \|p - \gamma u_{1_x} - q_h\|^2_{L^2(\Omega)}.
\end{aligned}
\tag{3.2.24}
$$

By the triangle inequality and Young's inequality ($p = q = \frac{1}{2}$), one gets

$$
\begin{aligned}
&\|\nabla (\boldsymbol{u} - \boldsymbol{u}_h)\|^2_{L^2(\Omega)} + \frac{\gamma}{\nu} \|\nabla \cdot (\boldsymbol{u} - \boldsymbol{u}_h)\|^2_{L^2(\Omega)} \\
&\leqslant 2\|\nabla \boldsymbol{\eta}\|^2_{L^2(\Omega)} + 2\|\nabla \boldsymbol{\phi}_h\|^2_{L^2(\Omega)} + \frac{2\gamma}{\nu} \|\nabla \cdot \boldsymbol{\eta}\|^2_{L^2(\Omega)} + \frac{2\gamma}{\nu} \|\nabla \cdot \boldsymbol{\phi}_h\|^2_{L^2(\Omega)}.
\end{aligned}
\tag{3.2.25}
$$

Plug the estimate (3.2.24) into (3.2.25), it gives the final result

$$
\begin{aligned}
\|\nabla (\boldsymbol{u} - \boldsymbol{u}_h)\|^2_{L^2(\Omega)} + \frac{\gamma}{\nu} \|\nabla \cdot (\boldsymbol{u} - \boldsymbol{u}_h)\|^2_{L^2(\Omega)} &\leqslant \left(6 + \frac{4\gamma^2}{\nu^2}\right) \|\nabla \boldsymbol{\eta}\|^2_{L^2(\Omega)} \\
&+ \frac{2\gamma}{\nu} \|\nabla \cdot \boldsymbol{\eta}\|^2_{L^2(\Omega)} + \frac{2}{\gamma \nu} \inf_{q_h \in Q_h} \|p - \gamma u_{1_x} - q_h\|^2_{L^2(\Omega)}.
\end{aligned}
\tag{3.2.26}
$$

■

Remark 3.2.4 Let $(\boldsymbol{u}, p)$ be the solution of (2.2.5), and the discrete Stokes equation (2.2.26) is solved by the grad-div stabilization method with Taylor-Hood pairs. If $V_{h,0}$ has optimal approximation properties, we have that

$$
\begin{aligned}
&\|\nabla (\boldsymbol{u} - \boldsymbol{u}_h)\|^2_{L^2(\Omega)} + \frac{\gamma}{\nu} \|\nabla \cdot (\boldsymbol{u} - \boldsymbol{u}_h)\|^2_{L^2(\Omega)} \\
&\qquad \leqslant C h^{2k} \left(\left(1 + \frac{\gamma}{\nu}\right) |\boldsymbol{u}|^2_{k+1} + \frac{1}{\nu \gamma} |p - \gamma u_{1_x}|^2_k \right).
\end{aligned}
\tag{3.2.27}
$$

Proof: The proof closely resembles that of Theorem 3.2.1 until reaching equation (3.2.20). Then, we take the $\boldsymbol{v}_h \in V_{h,0}$, since $\nabla \cdot \boldsymbol{\eta} = 0$, for the operator g, it gives

$$|\gamma g(\eta, \boldsymbol{v}_h)| = |\gamma(\eta_{1_x}, \nabla \cdot \boldsymbol{\phi}_h)| \leqslant \frac{\gamma}{4}\|\nabla \cdot \boldsymbol{\phi}_h\|^2_{L^2(\Omega)} + 2\gamma\|\nabla \boldsymbol{\eta}\|^2_{L^2(\Omega)}. \tag{3.2.28}$$

The first and third terms on the right-hand side of (3.2.20) are bounded as

$$\begin{aligned} |\nu(\nabla \boldsymbol{\eta}, \nabla \boldsymbol{\phi}_h)| &\leqslant \nu\|\nabla \boldsymbol{\eta}\|_{L^2(\Omega)}\|\nabla \boldsymbol{\phi}_h\|_{L^2(\Omega)} \\ &\leqslant \frac{\nu}{2}\|\nabla \boldsymbol{\eta}\|^2_{L^2(\Omega)} + \frac{\nu}{2}\|\nabla \boldsymbol{\phi}_h\|^2_{L^2(\Omega)}, \end{aligned} \tag{3.2.29}$$

and

$$\begin{aligned} |(\nabla \cdot \boldsymbol{\phi}_h, p - \gamma u_{1_x} - q_h)| &\leqslant \|\nabla \cdot \boldsymbol{\phi}_h\|_{L^2(\Omega)}\|p - \gamma u_{1_x} - q_h\|_{L^2(\Omega)} \\ &\leqslant \frac{\gamma}{4}\|\nabla \cdot \boldsymbol{\phi}_h\|^2_{L^2(\Omega)} + \frac{1}{\gamma}\|p - \gamma u_{1_x} - q_h\|^2_{L^2(\Omega)}. \end{aligned} \tag{3.2.30}$$

Combining these with (3.2.28), the final estimate is

$$\begin{aligned} \|\nabla(\boldsymbol{u} - \boldsymbol{u}_h)\|^2_{L^2(\Omega)} + \frac{\gamma}{\nu}\|\nabla \cdot (\boldsymbol{u} - \boldsymbol{u}_h)\|^2_{L^2(\Omega)} &\leqslant \left(4 + \frac{8\gamma}{\nu}\right)\|\nabla \boldsymbol{\eta}\|^2_{L^2(\Omega)} \\ &+ \frac{4}{\nu\gamma}\|p - \gamma u_{1_x} - q_h\|^2_{L^2(\Omega)}. \end{aligned} \tag{3.2.31}$$

Then, one applies standard approximation theory to get (3.2.27). ■

Remark 3.2.5 It is commonly observed that the sparse grad-div stabilization parameter reduces the impact of pressure on the velocity error, especially for scenarios where pressures are large and complex relative to velocities, and viscosities are small. Additionally, a value of $\gamma = \mathcal{O}(1)$ is often considered a suitable choice in terms of error scaling with respect to γ in [21]. □

Remark 3.2.6 The standard and sparse grad-div stabilizations have been introduced in the projection method for solving the Navier-Stokes equations, as studied in [17]. Error estimates for the velocity field in the unstabilized, standard grad-div stabilized, and sparse grad-div stabilized projection methods have been derived. These estimates demonstrate that either of the stabilized methods can significantly reduce the error, as the divergence term contributes a significant portion to the total error, which is supported by numerical evidence. In addition, both stabilized methods reduce the divergence error and yield more accurate solutions than the unstabilized method, thereby improving the conservation of mass to some extent. To delve deeper into these two stabilized methods, let the stabilization parameter γ be set as 1, and the Bicgstab method is used to solve the linear systems with different preconditions (Jacobi, Gauss-Seidel, and approximate block Gauss-Seidel with varying levels of accuracy). According to the numerical results, the sparse grad-div stabilization reveals a slight improvement over the standard grad-div method in terms of the number of iterations required to converge, as well as a reduction in the average iteration time of approximately 20% due to the sparser matrix structure. $\square$

Chapter 4

Numerical Studies

This section focuses on presenting the numerical results obtained from a set of 2D and 3D examples with known solutions. The aim is to compare the performance of the proposed stabilized methods, including standard grad-div stabilization and sparse grad-div stabilization, against the unstabilized method. Error estimates are also supported for the various methods. Additionally, the impact of the grad-div stabilization parameter on the velocity divergence error is analyzed. The section proceeds by exploring the characteristics of different Taylor-Hood finite element spaces with the standard grad-div method, and the influence of different values of viscosity ν on the numerical solutions of the 2D example. Finally, the efficiency of the two grad-div stabilization methods is compared through computations performed on a 3D example with analytical solutions. The simulations were performed with the code MooNMD [22].

4.1 2D Example

The two-dimensional problem we consider is a steady-state example with the exact solution as Example D.3 in [5] on the unit square domain $\Omega = (0,1)^2$ with homogeneous Dirichlet boundary conditions $\boldsymbol{u} = \mathbf{0}$ on $\partial\Omega$. The velocity field is defined using the stream function

$$\phi = 1000x^2(1-x)^4y^3(1-y)^2,$$

and given by

$$\boldsymbol{u} = \begin{pmatrix} u_1 \\ u_2 \end{pmatrix} = \begin{pmatrix} \partial_y\phi \\ -\partial_x\phi \end{pmatrix} = 1000 \begin{pmatrix} x^2(1-x)^4y^2(1-y)(3-5y) \\ -2x(1-x)^3(1-3x)y^3(1-y)^2 \end{pmatrix}. \quad (4.1.1)$$

The velocity is divergence-free which can be verified by the Theorem of Schwarz as follows

$$\nabla \cdot \boldsymbol{u} = \partial_x u_1 + \partial_y u_2 = \partial_{xy}\phi - \partial_{yx}\phi = \partial_{xy}\phi - \partial_{xy}\phi = 0.$$

Based on the boundary conditions, the pressure must be in $L_0^2(\Omega)$. In this case, the pressure was chosen as

$$p = \pi^2(xy^3cos(2\pi x^2y) - x^2ysin(2\pi xy)) + \frac{1}{8}. \tag{4.1.2}$$

4.1.1 Error Comparision of Different Grad-Div Stabilization Methods

The approximations for the prescribed solution (4.1.1) and (4.1.2) are computed for $\nu = 1$, using the unstabilized method (i.e., $\gamma = 0$), standard grad-div stabilization (i.e., $\gamma = 1$) and sparse grad-div stabilization method (i.e., $\gamma = 1$, based on u_{1_x}) in the finite element spaces P_2/P_1 of Taylor–Hood pair. Due to the necessity of the modified pressure in the sparse grad-div stabilization method, we will restrict our attention to velocity errors.
Figure 4.1 shows that all velocity errors have the orders of convergence as predicted in the numerical analysis. While no significant difference exists among the velocity errors obtained by using different methods in general, some variations on the coarse levels are noticeable in Figure 4.1c. Then, the different stabilization parameters are chosen to compare the divergence velocity error using P_2/P_1 Taylor-Hood pairs in different methods in Figure 4.2. It is evident that, with large parameters, both two stabilization methods show good performance in minimizing the divergence error of velocity, which improves the issue of mass conservation on coarse grids. However, as the mesh is refined, this effect weakens gradually.
Since the simulation results are so close, the standard grad-div stabilization with parameter $\gamma = 1$ is elected to show the magnitude of the velocity approximation on level 5 for the 2D example in Figure 4.3. As can be seen, the velocity field is essentially composed of one large vortex, and it is exactly zero at the boundary.

4.1.2 Comparison of Different Degrees of the Taylor-Hood Spaces

In this section, we use two different Taylor-Hood finite element spaces, namely P_3/P_2 and P_2/P_1, on successively refined irregular triangular meshes from Figure 4.4 to approximate the solution of the 2D example given by equations

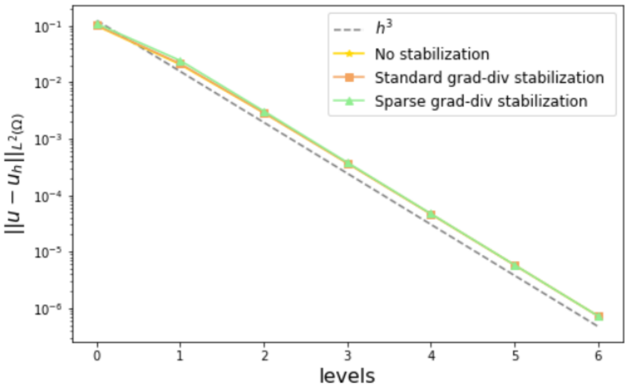

(a)

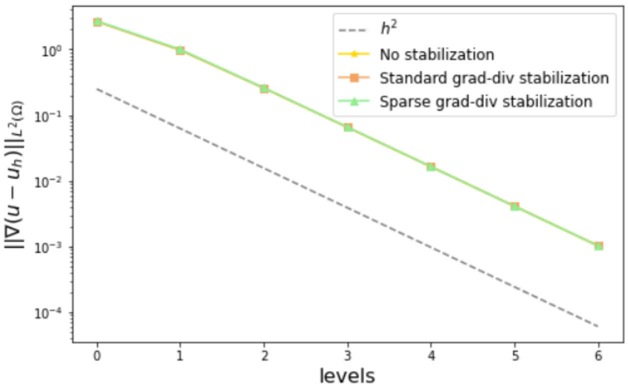

(b)

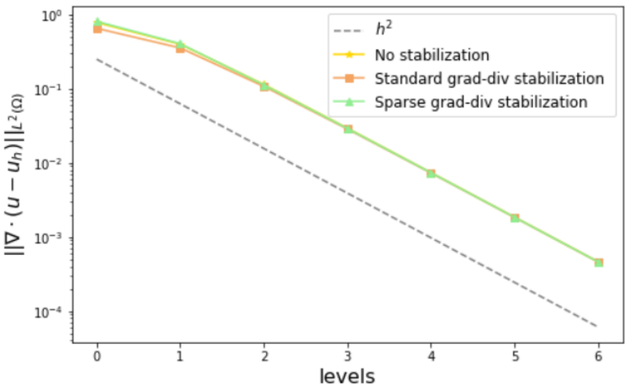

(c)

Figure 4.1: The L^2-norm of velocity error (a), the gradient velocity error (b), and the divergence velocity error (c) on different levels for the 2D problem

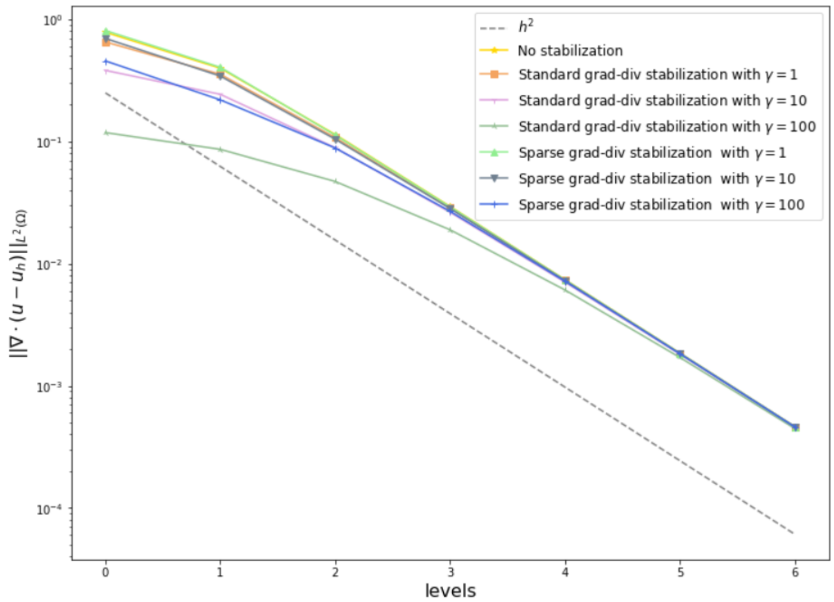

Figure 4.2: The divergence error with different methods and values of stabilization parameter

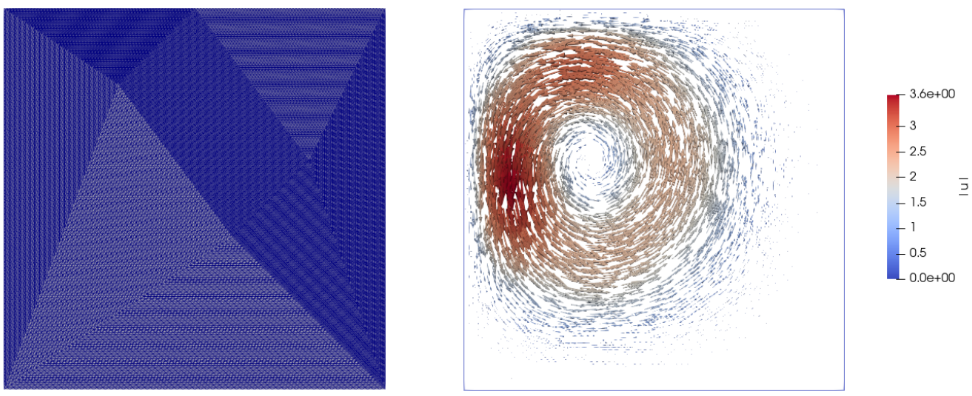

Figure 4.3: 2D example. Grid (left) and velocity (right) were solved by the standard grad-div stabilization method on level 5

(4.1.1) and (4.1.2) with $\nu = 1$.
Table 4.1 summarizes the comparison of the degrees of freedom, the velocity error in the L^2 norm, and the convergence order between the two different finite element spaces. It is apparent from the table that the P_3/P_2 space exhibits higher numerical accuracy and convergence order than the P_2/P_1 space. However, the former requires more degrees of freedom than the latter. Therefore, solving large-scale problems using P_3/P_2 space will demand more computational resources and time.

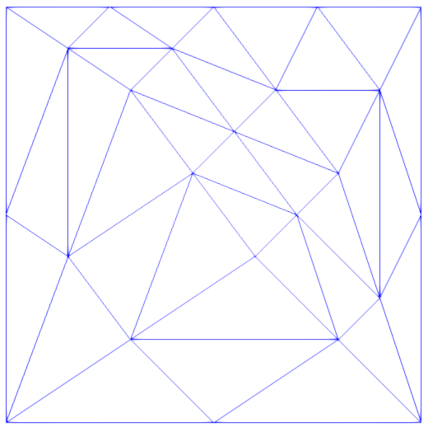

Figure 4.4: Initial irregular grid

Table 4.1: Degrees of freedom (dof), the velocity error in the L^2 norm ($\|\boldsymbol{u} - \boldsymbol{u_h}\|_{L^2(\Omega)}$) and convergence order (Rate) in different spaces

P_2/P_1			P_3/P_2		
dof	$\|\boldsymbol{u} - \boldsymbol{u_h}\|_{L^2(\Omega)}$	**Rate**	**dof**	$\|\boldsymbol{u} - \boldsymbol{u_h}\|_{L^2(\Omega)}$	**Rate**
190	1.02E-01		439	3.20E-02	
701	2.14E-02	2.2568141	1667	2.22E-03	3.84825958
2695	2.91E-03	2.87908082	6499	1.44E-04	3.95049914
10571	3.71E-04	2.97298003	25667	8.99E-06	3.99732877
41875	4.66E-05	2.99293779	102019	5.63E-07	3.99721235
166691	5.84E-06	2.99784403	406787	3.53E-08	3.99702323
665155	7.30E-07	2.99923684	1624579	2.21E-09	3.99790089

4.1.3 Comparison of Different Values of the Viscosity

We have obtained error estimates of the following form: (2.2.48) for the unstabilized method, (3.1.17) for the standard grad-div stabilization method, and (3.2.27) for the sparse grad-div stabilization method. All three error estimates are in particular for the P_2/P_1 Taylor-Hood space and with the inclusion of the viscosity term ν^{-1}. Therefore, we choose different values of viscosity to investigate its relationship with velocity errors in different methods. It is expected that as ν becomes small, the velocity errors will increase. Figure 4.5 shows the representative results obtained using the Taylor-Hood finite element space P_2/P_1 on the unstructured grid in Figure 4.4 with different methods. The visibility of the dependency of velocity errors on ν^{-1} is apparent. The velocity error decreases with large ν as predicted. However, the strength of this effect significantly weakens, when the value of viscosity increases to a certain degree. In general, the three methods exhibit good convergence properties with respect to the velocity errors of the solution for the 2D examples. However, both grad-div stabilization methods typically have smaller errors in the solution approximation than the unstabilized method with a small value of viscosity (i.e., $\nu = 10^{-5}$).

4.2 3D Example

Let $\Omega = (0,1)^3$ be a domain and consider a family of velocity and pressure fields as follows:

$$\boldsymbol{u} = \begin{pmatrix} u_1 \\ u_2 \\ u_3 \end{pmatrix} = \begin{pmatrix} f(x)\partial_y g(y)h(z) + f(x)g(y)\partial_z h(z) \\ -\partial_x f(x)g(y)h(z) + f(x)g(y)\partial_z h(z) \\ -\partial_x f(x)g(y)h(z) - f(x)\partial_y g(y)h(z) \end{pmatrix}, \tag{4.2.1}$$

with

$$f(x) = sin^2(\pi x),\ g(y) = sin^2(2\pi y),\ h(z) = z^2(1-z)^2$$

and

$$p(x) = 3x - sin(y + 4z) + C, \tag{4.2.2}$$

where the constant C has to be chosen so that the integral mean of p vanishes under Dirichlet boundary conditions at $\partial\Omega$. The approximations computed by the sparse grad-div stabilization method in P_2/P_1 Taylor-Hood finite element space are shown in Figure 4.6.

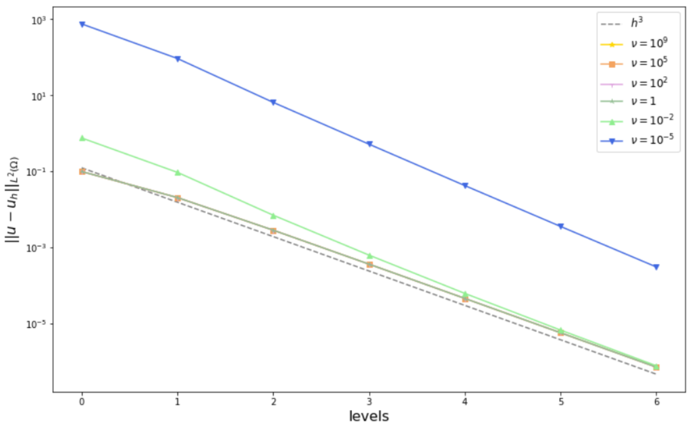

(a)

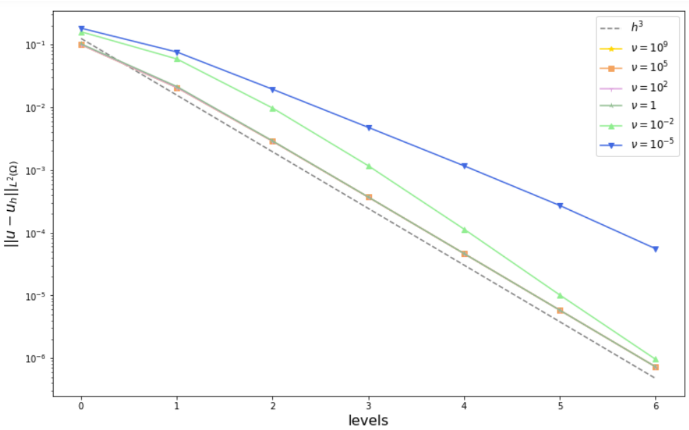

(b)

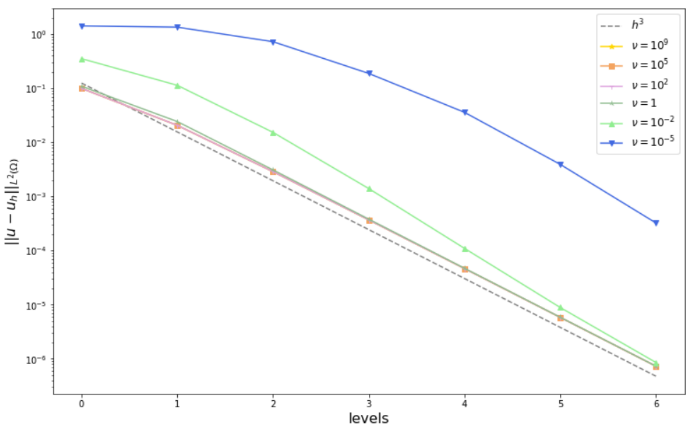

(c)

Figure 4.5: 2D Example. The L^2-norm of the velocity error with different values of viscosity using the unstabilized method (a), standard grad-div stabilization method with $\gamma = 1$ (b), and sparse grad-div stabilization method with $\gamma = 1$ (c)

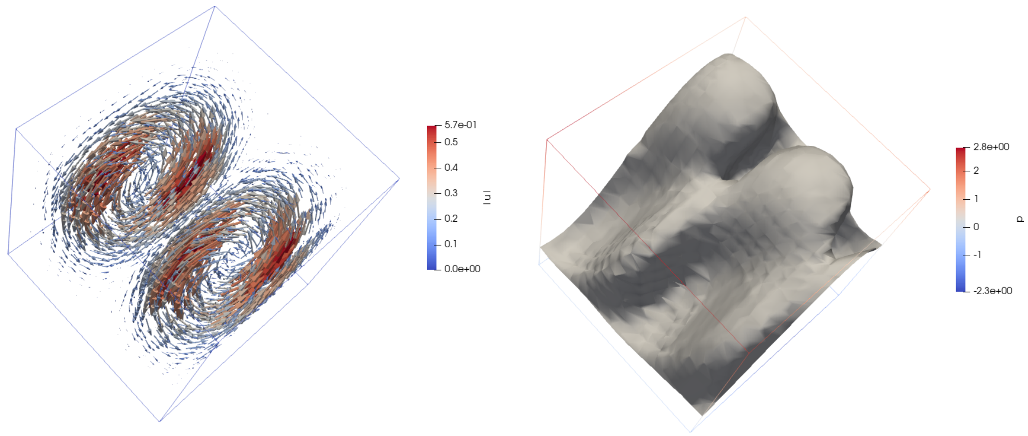

(a) (b)

Figure 4.6: 3D Example. The solution of velocity (a) and pressure (b) on level 3

4.2.1 Efficiency of Different Grad-Div Methods in 3D Example

The main advantage of the sparse grad-div stabilization method over the standard is that the linear system matrix can be explicitly decoupled as we mentioned before. Thus, the standard grad-div stabilization and sparse grad-div stabilization (based on u_{3_z}) are used in solving a same 3D problem with solution (4.2.1) and (4.2.2) in the P_2/P_1 Taylor-Hood space. The parameter γ and the value of viscosity ν are set as 1 for both stabilized methods, then the computation time for each level that uses the geometric multigrid solver of MooNMD is compared in Table 4.2. It is obvious that the computational advantage of the sparse grad-div method becomes more prominent, as the grid is refined.

Table 4.2: 3D example. Solve time for the sparse and standard grad-div stabilized method

Level	Solve time for sparse grad-div	Solve time for standard grad-div
0	0.215996	0.186439
1	2.42281	2.50395
2	33.3776	36.6226
3	404.782	436.483
4	3190.02	3492.43

Chapter 5

Summary

In this thesis, the existence and uniqueness of solutions to the Stokes equations were proved. We proposed different grad-div stabilization methods to improve the mass conservation of the solution and estimated the error and convergence rate of these methods.
The errors were compared in the 2D example for three different methods, namely unstabilized, standard grad-div stabilization, and sparse grad-div stabilization, which all demonstrated good convergence rates. We also found that the addition of the grad-div stabilization term can decrease the error of the divergence of the velocity, especially on coarser grids. However, as the grid became finer, the reduction of the divergence velocity error was less significant. Additionally, we found that a higher-order Taylor-Hood finite element space resulted in more accurate solutions but with higher computational costs. Further investigation was the sensitivity of the velocity error to the value of viscosity and found that all methods decreased the velocity error as the viscosity increased. But, this reduction became less significant at a certain point. Moreover, for small viscosity values, the velocity errors of the two grad-div stabilization methods are significantly smaller than those of the unstabilized method. Finally, we have compared the efficiency of the sparse grad-div stabilization method with that of the standard grad-div stabilization method in the 3D example and found that the sparse way is more efficient.
In conclusion, the grad-div method has been shown to be effective in improving the mass conservation of solutions, particularly when the viscosity value is small or the grad-div stabilization parameter is large. The sparse method is also a more efficient approach than the standard grad-div method.
The comparison of velocity errors for the three methods in the first part of the numerical study did not show clear differences, which may be due to the limited complexity of the test example. This suggests that further research is

needed to explore more complex scenarios. Specifically, concerning the selection of the grad-div stabilization parameters for different values of viscosity, we did not investigate their optimal range. Therefore, future research can delve into this issue, particularly in more complex models, to obtain more universal conclusions.

Bibliography

[1] A. J. Chorin and J. E. Marsden. *A mathematical introduction to fluid mechanics.*, volume 4 of *Texts Appl. Math.* New York etc.: Springer-Verlag, 2nd ed. edition, 1990.

[2] Lin Mu and Xiu Ye. A simple finite element method for the Stokes equations. *Adv. Comput. Math.*, 43(6):1305–1324, 2017.

[3] Lawrence C. Evans. *Partial differential equations*, volume 19 of *Grad. Stud. Math.* Providence, RI: American Mathematical Society (AMS), 2nd ed. edition, 2010.

[4] Vivette Girault and Pierre-Arnaud Raviart. *Finite element methods for Navier-Stokes equations. Theory and algorithms.*, volume 5 of *Springer Ser. Comput. Math.* Springer, Cham, (Extended version of the 1979 publ.) edition, 1986.

[5] Volker John. *Finite element methods for incompressible flow problems*, volume 51 of *Springer Ser. Comput. Math.* Cham: Springer, 2016.

[6] C. Taylor and P. Hood. A numerical solution of the Navier-Stokes equations using the finite element technique. *Comput. Fluids*, 1:73–100, 1973.

[7] Daniele Boffi, Franco Brezzi, and Michel Fortin. *Mixed finite element methods and applications*, volume 44 of *Springer Ser. Comput. Math.* Berlin: Springer, 2013.

[8] Howard C. Elman, David J. Silvester, and Andrew J. Wathen. *Finite elements and fast iterative solvers. With applications in incompressible fluid dynamics.* Numer. Math. Sci. Comput. Oxford: Oxford University Press, 2nd ed. edition, 2014.

[9] Maxim A. Olshanskii and Arnold Reusken. Grad-div stablilization for Stokes equations. *Math. Comput.*, 73(248):1699–1718, 2004.

[10] Maxim Olshanskii, Gert Lube, Timo Heister, and Johannes Löwe. Grad-div stabilization and subgrid pressure models for the incompressible Navier-Stokes equations. *Comput. Methods Appl. Mech. Eng.*, 198(49-52):3975–3988, 2009.

[11] Eleanor W. Jenkins, Volker John, Alexander Linke, and Leo G. Rebholz. On the parameter choice in grad-div stabilization for the Stokes equations. *Adv. Comput. Math.*, 40(2):491–516, 2014.

[12] Leopoldo P. Franca and Thomas J. R. Hughes. Two classes of mixed finite element methods. *Comput. Methods Appl. Mech. Eng.*, 69(1):89–129, 1988.

[13] William Layton, Carolina C. Manica, Monika Neda, Maxim Olshanskii, and Leo G. Rebholz. On the accuracy of the rotation form in simulations of the Navier-Stokes equations. *J. Comput. Phys.*, 228(9):3433–3447, 2008.

[14] Douglas N. Arnold, Richard S. Falk, and Ragnar Winther. Finite element exterior calculus, homological techniques, and applications. *Acta Numerica*, 15:1–155, 2006.

[15] Susanne C. Brenner and L. Ridgway Scott. *The mathematical theory of finite element methods*, volume 15 of *Texts Appl. Math.* New York, NY: Springer, 3rd ed. edition, 2008.

[16] Hans Petter Langtangen and Anders Logg. *Solving PDEs in Python. The FEniCS tutorial I*, volume 3 of *Simula SpringerBriefs Comput.* Cham: Springer Open, 2016.

[17] Abigail L. Bowers, Sabine Le Borne, and Leo G. Rebholz. Error analysis and iterative solvers for Navier-Stokes projection methods with standard and sparse grad-div stabilization. *Comput. Methods Appl. Mech. Eng.*, 275:1–19, 2014.

[18] Alexander Linke and Leo G. Rebholz. On a reduced sparsity stabilization of Grad-div type for incompressible flow problems. *Comput. Methods Appl. Mech. Eng.*, 261-262:142–153, 2013.

[19] P. M. Gresho and R. L. Sani. *Incompressible flow and the finite element method. Advection-diffusion and isothermal laminar flow. In collaboration with M. S. Engelman.* Chichester: Wiley, 1998.

[20] Sabine Le Borne and Leo G. Rebholz. Preconditioning sparse grad-div/augmented Lagrangian stabilized saddle point systems. *Comput. Vis. Sci.*, 16(6):259–269, 2013.

[21] Naveed Ahmed, Alexander Linke, and Christian Merdon. Towards pressure-robust mixed methods for the incompressible Navier-Stokes equations. *Comput. Methods Appl. Math.*, 18(3):353–372, 2018.

[22] Volker John and Gunnar Matthies. MooNMD – a program package based on mapped finite element methods. *Comput. Vis. Sci.*, 6(2-3):163–170, 2004.